Australian Government
Department of Defence
Defence Science and
Technology Organisation

An Assessment of the Usefulness of Water Tunnels for Aerodynamic Investigations

Lincoln P. Erm[1] and Michael V. OL[2]

[1]Air Vehicles Division,
Defence Science and Technology Organisation

[2]United States Air Force Research Laboratory

DSTO-TR-2803

ABSTRACT

Water tunnels are emerging as a possible useful alternative to small low-speed wind tunnels for an expanded range of aerodynamic testing. In this report, an assessment is made regarding the extent to which water tunnels can be used for such testing. It was found that their suitability for testing given models needs to be assessed on a case-by-case basis. For conventional tests on aircraft, such as force and moment measurements, they compare unfavourably with similar-sized wind tunnels, due to a mismatch in Reynolds numbers. Water tunnels are generally better suited to carrying out fundamental research than they are for applied aerodynamics testing. However, they are very useful as part of a large research program, by helping establish the testing schedule for large wind tunnels. In flow situations that are insensitive to Reynolds number, or where a test Reynolds number is close to that of a full-size vehicle, water tunnels should be regarded as the preferred option for experimental aerodynamics. Such examples include micro air vehicles, high-rate dynamic testing, and high-sweep sharp-edge configurations. Water tunnels are also very useful for providing validation data for computational-fluid-dynamics analyses of a flow. An earlier version of this work was prepared for the TTCP TR-AER-TP5 Panel in August 2010.

RELEASE LIMITATION

Approved for Public Release

Published by

Air Vehicles Division
DSTO Defence Science and Technology Organisation
506 Lorimer St
Fishermans Bend, Victoria 3207 Australia

Telephone: 1300 DEFENCE
Fax: (03) 9626 7999

© Commonwealth of Australia 2013
AR-015-530
December 2012

APPROVED FOR PUBLIC RELEASE

An Assessment of the Usefulness of Water Tunnels for Aerodynamic Investigations

Executive Summary

Water tunnels have some definite advantages over wind tunnels for aerodynamic testing of models. They are cheaper to build and operate, and simplified models can be easily modified to suit new testing requirements as a program proceeds. Water tunnels are ideally suited to flow-visualisation studies, giving an insight into the physics of the flow. With recent advances in measurement technology, they can now also be used to measure the very small flow-induced loads on models. Using water tunnels, it is possible to simultaneously measure loads and visualise high-quality off-surface flows, so that the loads and images can be correlated directly. Water tunnels are also better suited to modern laser-based flowfield-diagnostic methods, such as Particle Image Velocimetry. They are particularly amenable to dynamic testing because of the low rotation rates of models in water.

As with all testing in tunnels, similarity conditions ideally have to be satisfied to ensure that loads measured on models in tunnels can be scaled to correspond to full-size operation of a vehicle. Reynolds-number similarity is by far the most important similarity condition that must be satisfied, at least for low-velocity testing. Due to the small models and low free-stream velocities generally used in water tunnels, Reynolds numbers are typically at least three orders of magnitude less than those for full-size vehicles, such as aircraft. Therefore, water-tunnel data are only useful if this difference has no appreciable effects on flow patterns and the associated loads on models. Water tunnels are not useful for investigating flow problems at high Mach numbers, so the question of the usefulness of water tunnels for such flows was not addressed. The investigation is confined to low-subsonic flow regimes.

Although there are some definite advantages in using water tunnels rather than wind tunnels for aerodynamic investigations, the lack of Reynolds-number similarity is a major concern. There is little point using water tunnels for such investigations if the data are not meaningful. In this report, an assessment is made regarding whether water tunnels can now be used as a possible alternative to wind tunnels for an expanded range of aerodynamic testing.

It was found that the suitability of water tunnels for testing given models needs to be assessed on a case-by-case basis. Water tunnels will not overcome the need for large-scale, high-precision testing, and are at most marginally useful for producing reliable results in configuration aerodynamics, even in the conceptual design stage. For conventional aircraft testing, such as lift and drag measurements, they compare unfavourably with similar-sized wind tunnels, because of the mismatch in Reynolds numbers. Water tunnels are more of a fundamental research tool than an applied aerodynamics tool. However, they are very useful as a component of a large research program, by focusing the test matrix in large wind tunnels and providing validation for computational-fluid-dynamics analyses of the flow. In problems insensitive to Reynolds number, or where a test Reynolds number is close to that of a full-size vehicle, water tunnels should be regarded as the principal tool of experimental aerodynamics. Examples include micro air vehicles, high-rate dynamic testing, and high-sweep sharp-edge configurations.

Authors

Lincoln P. Erm
Air Vehicles Division

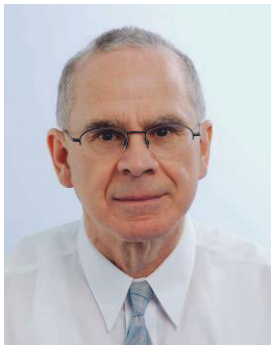

Lincoln Erm obtained a Bachelor of Engineering (Mechanical) degree in 1967 and a Master of Engineering Science degree in 1969, both from the University of Melbourne. His Master's degree was concerned with the yielding of aluminium alloy when subjected to both tensile and torsional loading. He joined the Aeronautical Research Laboratories (now called the Defence Science and Technology Organisation) in 1970 and has worked on a wide range of research projects, including the prediction of the performance of gas-turbine engines under conditions of pulsating flow, parametric studies of ramrocket performance, flow instability in aircraft intakes and problems associated with the landing of a helicopter on the flight deck of a ship. Concurrently with some of the above work, he studied at the University of Melbourne and in 1988 obtained his Doctor of Philosophy degree for work on low-Reynolds-number turbulent boundary layers. Since this time, he has undertaken research investigations in the low-speed wind tunnel and the water tunnel. Recent work has been concerned with extending the testing capabilities of the water tunnel, including developing a two-component strain-gauge-balance load-measurement system for the tunnel and developing a dynamic-testing capability for the tunnel.

Michael V. OL
United States Air Force Research Laboratory

Michael OL obtained his Bachelor of Aerospace Engineering (1992) and Master of Aerospace Engineering (1994) from the University of Michigan, and his Doctor of Philosophy degree (Aeronautics, 2001) from the California Institute of Technology. He has been employed at the U.S. Air Force Research Laboratory Aerospace Platforms Directorate since 1993, working primary on basic research related to unconventional subsonic aeronautical configurations, in particular small/micro unmanned air vehicles. His Ph.D. thesis was on vortex flows of nonslender delta wings, relating the stall process of such wings as a function of sweep and incidence angle. This work led him to problems in high angle of attack/separated flows and to unsteady aerodynamics, which is his current focus area. Dr. OL operates a water tunnel at AFRL, with a research group working on problems relating flowfield information to aerodynamic response, and to models useful for engineering design.

This page is intentionally blank

Contents

NOTATION

1. INTRODUCTION 1

2. PROPERTIES OF WATER AND AIR 2

3. SIMILARITY CONSIDERATIONS 3

4. BOUNDARY LAYERS ON MODELS AND FULL-SIZE VEHICLES 5

5. USE OF STRAIN-GAUGE BALANCES IN WATER TUNNELS 6

6. FLOW OVER AIRFOILS AND A THIN FLAT RECTANGULAR PLATE 6

7. FLOW OVER CIRCULAR-TYPE BODIES 9
7.1 Circular Cylinders 9
7.2 Tangent-Ogive Circular Bodies 11

8. FLOW OVER DELTA WINGS 14

9. FLOW OVER AN F/A-18 AIRCRAFT 19

10. DYNAMIC TESTING IN WATER TUNNELS 22

11. RAPID PROTOTYPING OF WATER-TUNNEL MODELS 29

12. LASER-BASED DISTRIBUTED-FLOWFIELD DIAGNOSTIC METHODS 29

13. EXAMPLE: PIV FOR A UCAV CONFIGURATION 29

14. GENERAL DISCUSSION AND CONCLUDING REMARKS 31

15. ACKNOWLEDGEMENTS 33

16. REFERENCES 34

This page is intentionally blank

Notation

AR	Aspect ratio of a rectangular flat plate.
a	Acoustic velocity (velocity of sound), (m·s^{-1}).
C_D	Drag-force coefficient.
C_{D0}	Drag-force coefficient for zero angle of attack.
C_L	Lift-force coefficient.
C_m	Pitching-moment coefficient.
$C_{mq} + C_{m\dot{\alpha}}$	Combined dynamic derivative for the pitching moment due to the effects of pitch rate and angle of attack rate.
$C_{m_{\delta e}}$	Static pitching-moment derivative with respect to elevator angle, $\partial C_m / \partial \delta_e$.
C_p	Pressure coefficient.
$C_{Y(max)}$	Maximum side-force coefficient.
C_Z	Normal-force coefficient.
c	Chord of a wing, (m).
D	Characteristic length scale, diameter of a cylinder, (m).
D	Drag force, (N).
Fr	Froude number, $Fr = U/(gD)^{0.5}$.
g	Acceleration due to gravity, (m·s^{-2}).
L	Centreline chord of a delta wing, length of F/A-18 aircraft, (m).
L	Lift force, (N).
M_t	Mach number, $M_t = U/a$.
p	Static pressure, (Pa).
Re, Re_D	Reynolds number, $Re = \rho UD/\mu$.
s	Local semispan of a delta wing, (m).
St	Strouhal number, $St = \omega D/U$.
U	Free-stream velocity, (m·s^{-1}).
u	Velocity in boundary layer, (m·s^{-1}).
$u'v'$	Kinematic Reynolds stress, (m^2·s^{-2}).
We	Weber number, $We = \rho U^2 D/\sigma$.
x	Distance along a flat plate from the leading edge, distance along a body from the nose, chordwise distance from the apex of a delta wing, (m).
y	Spanwise distance from the centreline chord of a delta wing, (m).
Z	Normal force acting on a model, (N).

Greek Letters

α	Angle of attack, (degrees).
δ_e	Angle of elevator on wing (degrees).
δ_L , δ_T	Laminar and turbulent boundary-layer thicknesses, (m).
θ	Pitch angle, (degrees).
θ_s	Angle defining the separation point on a cylinder, (degrees).
μ	Dynamic viscosity of a fluid, (kg·m^{-1}·s^{-1}).
ν	Kinematic viscosity of a fluid, (m^2·s^{-1}).
ρ	Density of a fluid, (kg·m^{-3}).
σ	Surface tension, (kg·s^{-2}).
τ	Surface shear stress on a body, $\tau = \mu\, \partial u/\partial y$, (N·m^{-2}).

ϕ	Phase of plunging motion.
ω	Vortex shedding frequency (from one side of a body), (s^{-1}).

Acronyms

BART	Basic Aerodynamic Research Tunnel, NASA Langley Research Center.
CFD	Computational Fluid Dynamics.
DSTO	Defence Science and Technology Organisation.
DTRC	David Taylor Research Center.
IAR	Institute of Aerospace Research.
JSF	Joint Strike Fighter.
MAV	Micro Air Vehicle.
McAir	McDonnell Aircraft Company.
NAE	National Aeronautical Establishment, Ottawa (Ontario).
OPLEC	Orbital Platform Rotary Balance System.
PIV	Particle Image Velocimetry.
SDM	Standard Dynamics Model.
TTCP	The Technical Cooperation Program.
UAV	Uninhabited Air Vehicle.

1. Introduction

In experimental science there is often a tension between small/cheap/simple/readily-accessible experimental apparatus on the one hand, and elaborate/detailed/complex/ expensive apparatus on the other hand. It is specious to claim that one is better than the other, as each enjoys its proper place in the spectrum from exploratory investigation of fundamentals to detailed engineering design. But it is possible to devise a metric of return on effort, or value for money, and on this basis one can find a very favourable result for water tunnels.

Water tunnels definitely belong to the first category in experimental aerodynamics, as almost universally they are of scale and scheme commensurate with what one finds in university laboratories, rather than showpieces of government or industry installations. They can generally be operated and maintained by one to two engineers with no special proficiency beyond general familiarity with fluid-mechanics measurements. Environmental impact and electrical power requirements are small (rarely > 50 kW), safety concerns are minimal (and generally overwhelmed by concerns for constituent equipment, such as lasers, rather than the facility itself), and facility availability is essentially continuous. Water-tunnel models can also be built quicker and cheaper than wind-tunnel models, and can easily be modified to satisfy new requirements as a testing program proceeds.

In the past, water tunnels have primarily been used to carry out detailed flow-visualisation studies using scaled models, such as aircraft. They are better suited to such studies than are wind tunnels, due to water having a higher density and lower mass diffusivity than air, and the fact that the free-stream velocities used in water tunnels are generally substantially less than those used in wind tunnels. Flow-visualisation can give an insight into the complex flow behaviour around models, enabling researchers to obtain an understanding of the fluid dynamics of the flow.

With the development of pressure-transducer and strain-gauge-balance technologies, it is now possible to measure accurately the very small flow-induced pressures, forces and moments on models in water tunnels. Loads can be measured while simultaneously visualising detailed flow patterns, so that the loads and the images can be correlated directly. This development potentially increases the usefulness of water tunnels. The explosive growth in laser-based distributed-flowfield diagnostic methods, such as Particle Image Velocimetry (PIV), provides a ready and powerful means of comparison with the equally fast-growing power of Computational Fluid Dynamics (CFD). Such methods are easier to apply in water than in air. The high density and dynamic viscosity of water relative to air (see Section 2) can potentially greatly simplify measurements in unsteady aerodynamics and in dynamic testing (see Section 10).

Water tunnels, like any facility, are not a panacea for low-cost solutions to complex engineering problems. In some situations water tunnels compare favourably with similarly-sized wind tunnels, whereas in other situations, chiefly where Reynolds-number and Mach-number scaling are important, water tunnels compare unfavourably. Water-tunnel testing is subject to severe limitations, principally due to unavoidably low Reynolds numbers and Mach

numbers. Also, there are complications in dealing with water -corrosion, leaks, requirements for water filtering and so forth, but these remain in-scope for small facilities in general.

It may now be possible for water tunnels to play a more important role in aerodynamic testing compared with previously. However, researchers need to proceed with caution. They need to know what types of models can be used in water tunnels and what types of tests can be undertaken to obtain meaningful results. There is no point carrying out experiments in water tunnels if the data are not useful. The main purpose of this paper is to address these questions.

The true promise of water tunnels cannot be fulfilled by water-tunnel specialists self-segregating into their narrow community of practitioners. Instead, it is important for water-tunnel users to work together with the CFD community and the large wind-tunnel community, for example in the areas of CFD validation and development of test matrices for large Test and Evaluation wind tunnels.

2. Properties of Water and Air

The properties of water and air at standard conditions are shown in Table 1. Corresponding properties between the two media differ substantially, which can have implications when carrying out research in fluid mechanics and aerodynamics. Water has a density over 800 times that of air and a dynamic viscosity which is over 50 times greater. The sonic velocity in water is over 4 times that in air.

Table 1. Properties of water and air at 20 °C and standard atmospheric pressure, 101325 Pa.

Property	Water	Air	Unit	Water/Air
Density	998.2	1.204	$kg \cdot m^{-3}$	829.1
Dynamic viscosity	1.002×10^{-3}	1.813×10^{-5}	$kg \cdot m^{-1} \cdot s^{-1}$	55.27
Kinematic viscosity	1.003×10^{-6}	1.506×10^{-5}	$m^2 \cdot s^{-1}$	0.0666
Sonic velocity	1482	343.2	$m \cdot s^{-1}$	4.318

For fundamental boundary-layer studies, properties of water are favourable compared with those for air. Turbulent Reynolds stresses, which are proportional to density, are over 800 times larger in water than in air, so that they can be measured more easily. The kinematic viscosity of water is about 15 times smaller than that for air, so that for aerodynamic studies, test Reynolds numbers in water are greater than those in air by this factor, for tests carried out using models of the same size and for the same free-stream velocity. However, this Reynolds-number advantage is lost in practice, since testing in air is usually done with substantially larger models and significantly higher free-stream velocities.

3. Similarity Considerations

Whenever models are tested in tunnels, an attempt is made to satisfy similarity requirements, so that the tunnel tests are representative of the operation of full-size vehicles. There are three levels of similarity that must be satisfied, namely geometric, kinematic and dynamic similarity. For geometric similarity, a model must have the same shape as a full-size vehicle, so that corresponding dimensions have a constant ratio. For kinematic similarity, velocities at corresponding locations in the flow fields must have a constant ratio. For dynamic similarity, forces at corresponding locations must have a constant ratio.

In typical fluid-flow problems, there are a number of variables that commonly arise. These include:

- D characteristic length scale, (m)
- U free-stream velocity, (m·s^{-1})
- p static pressure, (Pa)
- ρ density, (kg·m^{-3})
- μ dynamic viscosity, (kg·m^{-1}·s^{-1})
- g acceleration due to gravity, (m·s^{-2})
- ω vortex shedding frequency (from one side of a body), (s^{-1})
- a speed of sound, (m·s^{-1})
- σ surface tension, (kg·s^{-2})

Considering dynamic similarity, variables given above are generally arranged into non-dimensional groups which are given special names, as shown in Table 2.

Table 2. Dimensionless groups used when testing models, based on a table given by Munsen, Young & Okiishi, (2006).

Dimensionless Group	Name	Interpretation	Types of Applications
$\frac{\rho U D}{\mu}$	Reynolds number, *Re*	$\frac{\text{inertia force}}{\text{viscous force}}$	All types of fluid-dynamics flows
$\frac{U}{a}$	Mach number, M_t	$\frac{\text{flow speed}}{\text{speed of sound}}$ $\frac{\text{inertia force}}{\text{compressibility force}}$	Flows in which compressibility is important
$\frac{\omega D}{U}$	Strouhal number, *St*	$\frac{\text{wavelength}}{\text{length scale}}$ $\frac{\text{inertia (local) force}}{\text{inertia (convective) force}}$	Unsteady flows with a characteristic frequency of oscillation
$\frac{U}{\sqrt{gD}}$	Froude number, *Fr*	$\frac{\text{inertia force}}{\text{gravitational force}}$	Flows with a free surface
$\frac{\rho U^2 D}{\sigma}$	Weber number, *We*	$\frac{\text{inertia force}}{\text{Surface-tension force}}$	Flows in which surface tension is important

Each of these non-dimensional groups can be interpreted as the ratio of two physically-meaningful quantities, as shown. For example, the Reynolds number is often interpreted as the ratio of a typical inertia force on a fluid particle to a typical viscous force on the particle. Depending on the fluid-flow problem being considered, some or all of these forces could be important. If, for example, the full-size flow is affected by inertia, viscous, gravitational and surface-tension forces, then the Reynolds number, Froude number and Weber number for the model flow must all be the same as those for the full-size flow. In practice, it is often not possible to satisfy such a requirement. However, some of the forces may not be as important as others and can therefore be neglected, so that a partial similarity can be achieved, which may be sufficiently accurate.

The current study is only concerned with models that are fully submerged in water tunnels. For such setups, Reynolds-number similarity is by far the most important similarity condition that must be considered, and is the condition which researchers would like to satisfy. Although Mach-number similarity (compressibility) is important for some aerodynamic problems, such as shock/boundary-layer interactions, similarity clearly cannot be achieved in water tunnels, due to the low velocities involved –see Table 3. This point is generally obvious and is unlikely to cause errors in practice. If compressibility effects are important, then model tests should be carried out in a high-velocity wind tunnel. Strouhal-number similarity is important whenever vortices are systematically shed from bluff bodies, such as occurs when vortices are shed from the superstructure of a frigate, and then pass over its flight deck. Froude-number similarity is important when a model such as a ship is protruding through a free surface, and for free-flight dynamic testing, both of which are not currently being considered. Surface-tension forces are generally not important for the types of flow situations currently being considered, so that there is no need to consider Weber-number similarity.

In addition to the above similarity requirements, it is important that levels of free-stream turbulence are not mismatched between model flows and full-size flows, since this can affect measured parameters. This is often overlooked by researchers.

Table 3. Typical values of flow parameters for models and a full-size aircraft.

Testing Environment	**Reynolds Number*** $Re = \frac{\rho U D}{\mu}$	**Mach Number** $M_t = \frac{U}{a}$	**Dynamic Pressure** $0.5\rho U^2$ (Pa)
Water Tunnel	10^4 to 10^5	0.000067	5.0
Low Speed Wind Tunnel	2×10^6	0.2	2200
Transonic Wind Tunnel	5×10^6	0.6	24500
Full-Scale Flight	6×10^7	0.6	24500

* Reynolds numbers are based on mean aerodynamic chords.

Typical Reynolds numbers, Mach numbers and dynamic pressures for models in water and wind tunnels, and for a typical full-size combat aircraft, are shown in Table 3. There are clearly significant differences between corresponding flow parameters for the different cases.

The Reynolds number for tests on a model in a water tunnel is at least three orders of magnitude less than that for tests on a full-size vehicle. Due to practical difficulties of having constraints on tunnel size, model size and testing velocity, the requirement of Reynolds-number similarity is generally not achieved when testing models of combat aircraft, both for wind tunnels and water tunnels. The foregoing is the reality of testing in tunnels, and it is crucial that researchers are fully cognizant of the situation.

4. Boundary Layers on Models and Full-Size Vehicles

Boundary layers on full-size vehicles are generally predominantly turbulent whereas corresponding boundary layers on models in water tunnels are generally laminar. The thicknesses of incompressible turbulent and laminar boundary layers developing along flat plates at zero angle of attack are given by (see, for example, Anderson, 2005).

$$\delta_{\mathrm{T}} = \frac{0.37x}{Re_{\mathrm{x}}^{0.2}} \tag{1}$$

and

$$\delta_{L} = \frac{5.0x}{\sqrt{Re_{\mathrm{x}}}} \tag{2}$$

respectively. The thickness of a turbulent boundary layer half way along a full-size aircraft of length 17 m is about 122 mm (calculated using equation 1), whereas the thickness of a laminar boundary layer half way along a water tunnel model of length 0.354 m (1/48 size model) is about 15 mm (calculated using equation 2), i.e. the ratio of the thickness of the turbulent boundary layer to that of the laminar boundary layer is about 8:1. However, the thickness of the turbulent boundary layer on the full-size aircraft is about 0.7% of its length, whereas the thickness of the laminar boundary layer on the water tunnel model is about 4.2% of its length, so that the ratio of the scaled thickness of the laminar boundary layer to that of the turbulent boundary layer is about 6:1.

Normalised velocity profiles for laminar and turbulent boundary layers differ significantly. Surface shear stresses, given by $\tau = \mu \partial u/\partial y$, differ markedly for models in a water tunnel and for full-size aircraft, due to the differences in the velocity profiles for laminar and turbulent layers, and because of the different dynamic viscosities for water and air (see Table 1). Scaled tangential skin-friction forces on the surface of a model enveloped in a laminar boundary layer are substantially less than those on a full-size aircraft enveloped in a turbulent boundary layer, so that scaled drag forces measured on water-tunnel models are therefore not representative of those on full-size aircraft.

For wind-tunnel models, a tripping device is often attached to a model to cause transition from laminar to turbulent flow. Ideally, the salient features of boundary layers on models in tunnels will then be similar to those on full-size aircraft. Such devices are often a row of cylindrical pins or a strip of distributed roughness (such as sandpaper). However, the effectiveness of tripping devices on wind-tunnel models is questionable for complex three-

dimensional flows, especially for aircraft models undergoing dynamic manoeuvres. Fisher & Cobleigh (1994) and Kramer *et al*. (1994) indicate that that the use of tripping devices on water-tunnel models to artificially create a desired boundary-layer condition is unlikely to be effective since laminar separation would most likely occur, rather than transition to turbulent flow.

5. Use of Strain-Gauge Balances in Water Tunnels

With the development of strain-gauge technology, it is now possible to manufacture strain-gauge balances to measure the very small flow-induced forces and moments on models in water tunnels. Both a two-component and a five-component balance have been designed and built at the Defence Science and Technology Organisation (DSTO) for use in a water tunnel -see Erm (2006a), Erm & Ferrarotto (2010). Due to the conductivity and corrosive properties of water, strain-gauge-balance design can be quite troublesome, as gauges need to be waterproofed. The waterproofing courts the possibility of balance fouling, and in any case is rarely robust. The gauges on the balances, prior to waterproofing, are shown in Figure 1. Due to the small loads, semi-conductor strain gauges have been used. The two-component balance has been designed to measure normal forces and pitching moments within the ranges ±2.5 N and ±0.02 N·m respectively. The five-component balance was designed to measure side and normal forces, as well as rolling, pitching and yawing moments, within the ranges ±25 N, ±25 N, ±0.1 N·m, ±0.2 N·m and ±0.2 N·m respectively.

Due to difficulties in obtaining meaningful longitudinal forces on water-tunnel models (see Section 4), there is no point measuring such forces using a strain-gauge balance. Water-tunnel balances are therefore usually restricted to five components, as also used by Suárez *et al.* (1994a) and Suarez & Malcolm (1994). By restricting balances to five components, it is therefore generally not possible to measure lift forces and drag forces on models, which are respectively normal to, and in the direction of, the free-stream velocity. This significantly reduces the usefulness of balances in water tunnels.

6. Flow Over Airfoils and a Thin Flat Rectangular Plate

The major impediment in usefulness of water tunnels for aerodynamic applications is from Reynolds-number scaling. Chord-based Reynolds numbers for airfoils, wings and aircraft models are typically limited in water tunnels to an upper-bound of 10^5. For whole-airplane configurations, Reynolds numbers based on mean aerodynamic chord can be limited to 10^4 for smaller water tunnels. For airfoil performance, and therefore airplane-performance measurements even at the conceptual-design level, this is a devastating and likely unacceptable limitation, since below $Re = 10^5$ most airfoils evince large laminar separations wholly unrepresentative of flight conditions or even large-wind-tunnel conditions, and at $Re \sim 10^4$ all airfoils operate in separated flow at all angles of attack. For $Re \sim 5 \times 10^4$ to 2.5×10^5, Reynolds numbers will be subcritical, and laminar separation bubbles will either be

very large or will be "open", resulting in the airfoil behaving something like a bluff body. This to some extent depends on the smoothness of the airfoil surface; "rough" airfoils are less Reynolds-number sensitive; refer to the classic airfoil performance cartoon by Horten shown in Figure 2, as reported by Mueller & DeLaurier (2001), which compares airfoil maximum lift to drag ratio across the Reynolds-number range, down to the range for insects. Drastic fall of maximum L/D is concurrent with large, open separations.

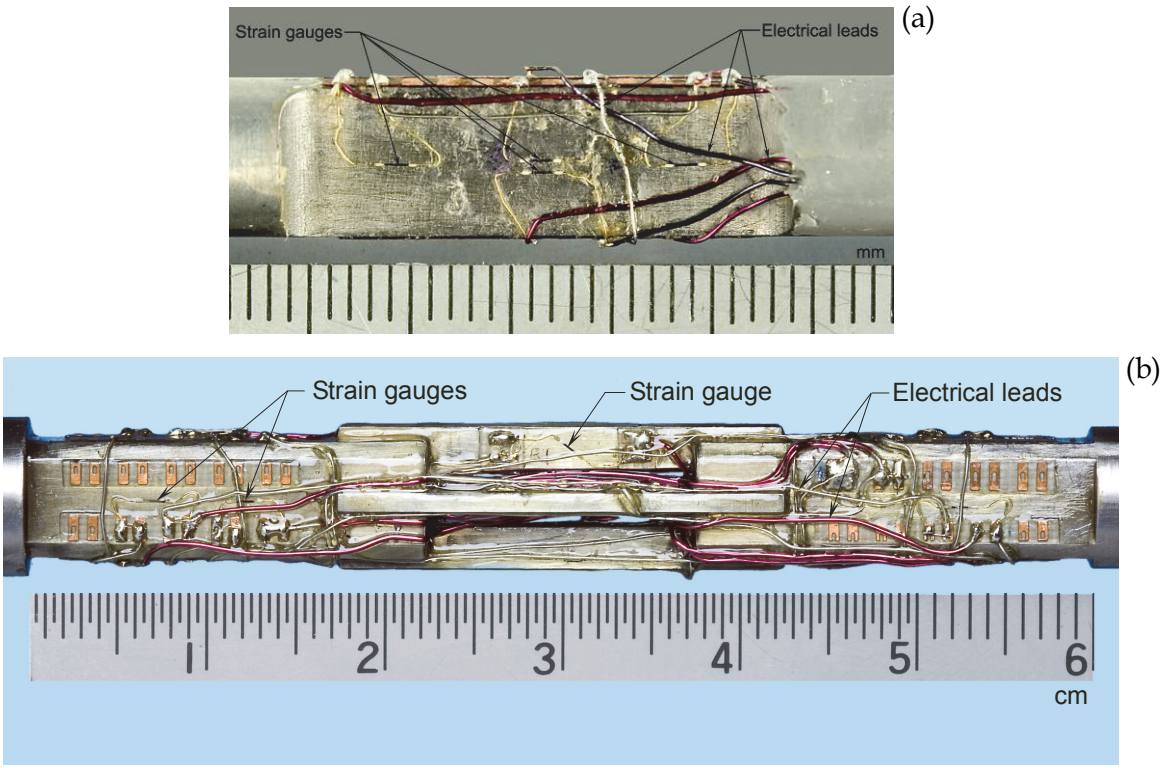

Figure 1. DSTO strain-gauge balances, showing gauges and leads, prior to waterproofing, (a) two-component balance, (b) five-component balance.

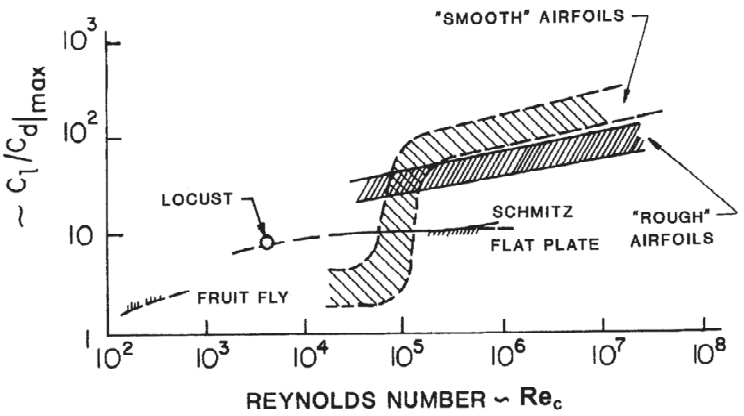

Figure 2. Notional estimate of airfoil performance vs. Reynolds number, from Horton, as reported by Mueller & DeLaurier (2001).

A more quantitative rendition of prototypical decline in airfoil performance is given in Figure 3, which shows what happens to airfoil drag polars in going from $Re = 5 \times 10^5$ down to 6×10^4. While C_{D0} doubles in going from $Re = 2 \times 10^5$ to 5×10^5, and certainly this is a problem for performance-type of aerodynamic testing, the far greater problem is the explosive growth in drag in going below $Re = 2 \times 10^5$.

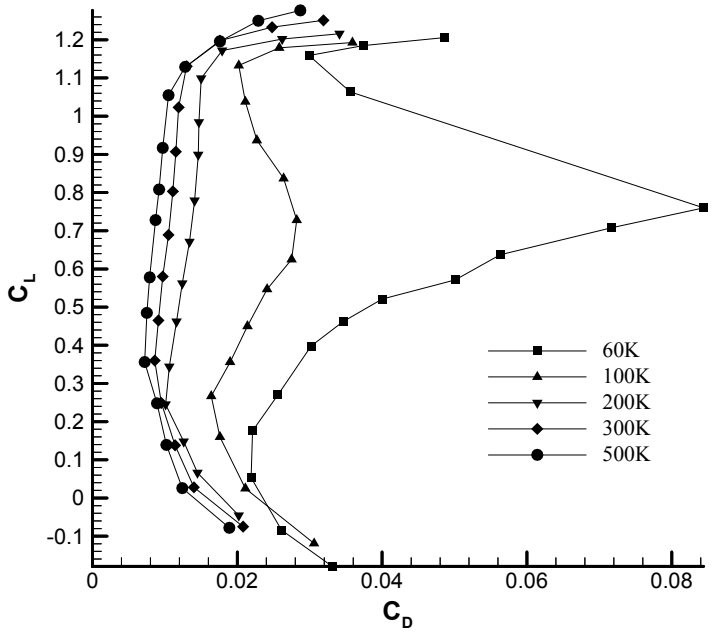

Figure 3. Eppler E387 airfoil drag polar, $Re = 6 \times 10^4$ to 5×10^5, collected from wind-tunnel data at the University of Illinois, Urbana-Champaign –see Selig (2006-2008).

Thus we have a qualitative, and not just a quantitative disparity between water-tunnel test conditions and flight (or large wind tunnel). There are other problems besides decline of airfoil performance at low Reynolds numbers. Control surface performance will be anomalous, so for example for a classical airplane configuration the $C_{m_{\delta e}}$ will be wrong. The stall dynamics will also be quite different. Wind tunnels of similar size (say, test section diameter of order 0.5 m) have an advantage of about a fivefold increase in airfoil sectional Reynolds number, which is enough to exceed the critical Reynolds number and therefore to at least qualitatively match the flight-like scenario, at least for angles of attack below stall. Referring to Figure 2, the small wind tunnel will still give a palpably overestimated C_{D0}, but should at least qualitatively capture the "correct" gross flowfield -whereas the water tunnel may not. Of course, for laminar-flow airfoils, all of these conclusions must be attenuated, and the better approach for performance testing would be to avoid small tunnels entirely, be they wind or water.

The foregoing suggests that it would be foolish to employ a water tunnel for airplane performance testing, for data such as lift-curve slope, stall angle, elevator-control power, trim-angle-of-attack range, C_{D0}, and so forth, even at the conceptual design level. Instead, one should do potential-flow computations with viscous corrections (such as XFOIL), and if necessary run RANS computations for C_{D0} and stall behaviour. One would appeal to experiment in water tunnels either upon finding anomalies or ambiguities in the computations, or in doing fundamental research prior to investigating applications to

airplanes. And water tunnels could be used as "pilot" facilities to guide test planning in larger wind tunnels, later in the design cycle.

A simple but convincing steady-aerodynamics example or Reynolds-number-insensitive flows is water-tunnel testing of a thin rectangular flat plate having an aspect ratio of 2 – see Figure 4 from Kaplan, Altman & Ol (2007). Between the low aspect ratio and the "sharp" leading edge, Reynolds-number-effects are attenuated to the point where the measured lift coefficient comports very well with classical *inviscid* theory. Further, lift coefficient from direct measurement via a force balance compares well with lift derived from Kutta-Joukowski treatment of the tip-vortex circulation in the Trefftz plane, obtained from PIV. The three-way comparison with theory holds well, up to stall. This implies that the term "Reynolds number insensitive" is neither a trite platitude nor a rare exception in flows of interest in applied aerodynamics. But certainly one must use caution!

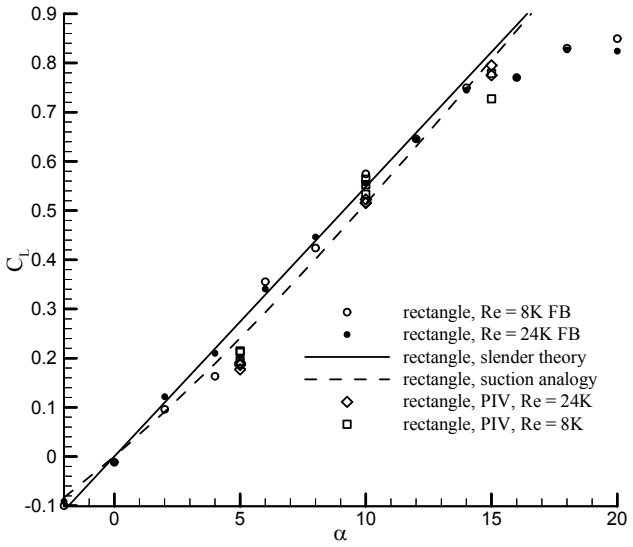

Figure 4. Lift coefficient vs. angle of attack for AR = 2 rectangular plate. Re = 8000 and 24,000; force balance data ("FB"), PIV data, and inviscid theory, –see Kaplan, Altman & Ol, (2007).

7. Flow Over Circular-Type Bodies

7.1 Circular Cylinders

The flow around a circular cylinder located at right angles to the oncoming flow can be used to qualitatively explain many Reynolds-number-dependent viscous-flow phenomena encountered by combat aircraft and missiles. Figure 5, adapted from Polhamus (1984), shows how the drag coefficient, C_D, varies with Reynolds number, $Re_D = \rho UD/\mu$, for a circular cylinder having its axis normal to the oncoming flow. The Reynolds number determines whether the boundary layer on the cylinder is laminar, transitional or turbulent, which in turn strongly influences the flow topology and loads on the cylinder. According to Polhamus, the flow can be divided into a number of different Reynolds-number ranges, namely the

subcritical, critical, supercritical and hypercritical ranges. The subcritical range corresponds to $Re_D \leq 2 \times 10^5$. In this range, laminar separation of the boundary layer occurs on the windward side of the cylinder at a separation angle, θ_s, of about 80°, which results in a wide wake and a relative large value of C_D. The critical range corresponds to $2 \times 10^5 \leq Re_D \leq 4 \times 10^5$ and $80° \leq \theta_s \leq 130°$ (approximate values). In this range, laminar separation is followed by turbulent reattachment, enclosing a laminar bubble, followed by turbulent separation, resulting in a narrowing of the wake and a large reduction in C_D. The supercritical range corresponds to $4 \times 10^5 \leq Re_D \leq 6 \times 10^6$ and $115° \leq \theta_s \leq 130°$ (approximate values). In this range, the transition and separation regions move upstream (θ_s decreases) and there is a corresponding increase in C_D.

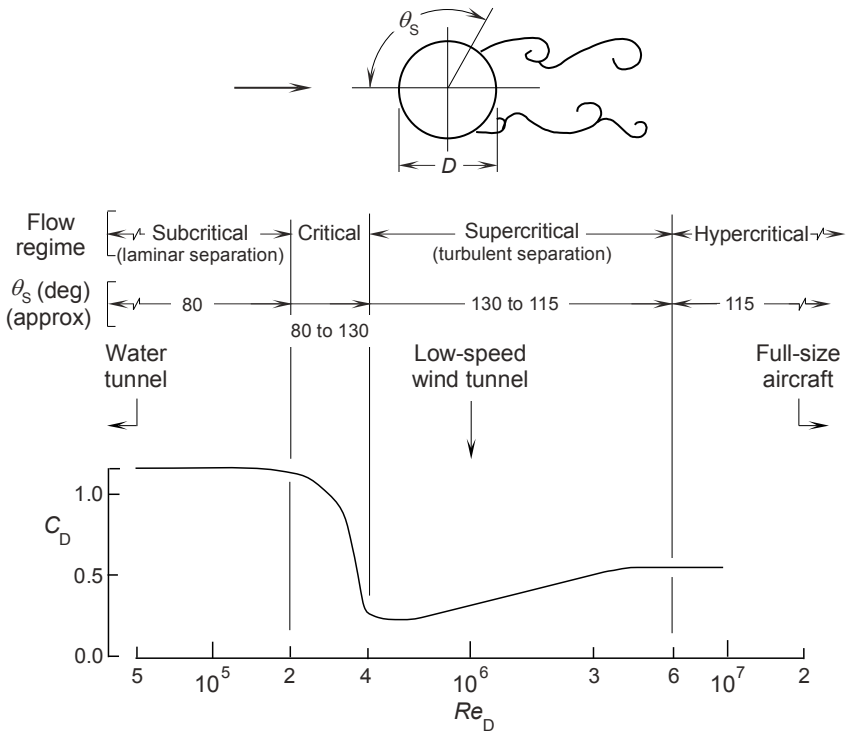

Figure 5. Variation of C_D on a cylinder in crossflow at different Reynolds numbers, based on a figure given by Polhamus (1984).

The flow in the wake of a circular cylinder is characterised by vortices of different frequencies, which are shed alternatively from both sides of the body. These vortices result in alternating forces on the body, particularly in a direction normal to the oncoming flow (see Section 7.2). It is well known that the vortex shedding frequency, expressed in terms of the Strouhal number, $St = \omega D/U$ (see Section 3), is dependent on the Reynolds number. This dependency, for a circular cylinder normal to the flow, is shown in Figure 6, adapted from Polhamus (1984), which contains data from different investigations. According to Polhamus, the behaviour of the vortex wake can be subdivided into different regions, depending on the Reynolds number, as shown. For the subcritical Reynolds-number range, the Strouhal number has a value of about 0.2 and vortices are shed into the wake at a dominant frequency, although they are not of the classical Karman type. For the critical range, where the laminar bubble with turbulent reattachment and separation is formed, the wake becomes narrow and is unstructured. The

vortex-shedding frequencies are of the "wide-band random" type with no dominant frequencies. In the lower part of the supercritical region, the vortex-shedding frequencies are still of the "wide-band random" type, with vortex shedding frequencies varying between two dominant values, corresponding to Strouhal numbers of about 0.2 and about 0.5. In the upper part of the supercritical region, the vortex shedding frequencies are of the 'narrow-band random" type, with Strouhal numbers reaching a value of about 0.3.

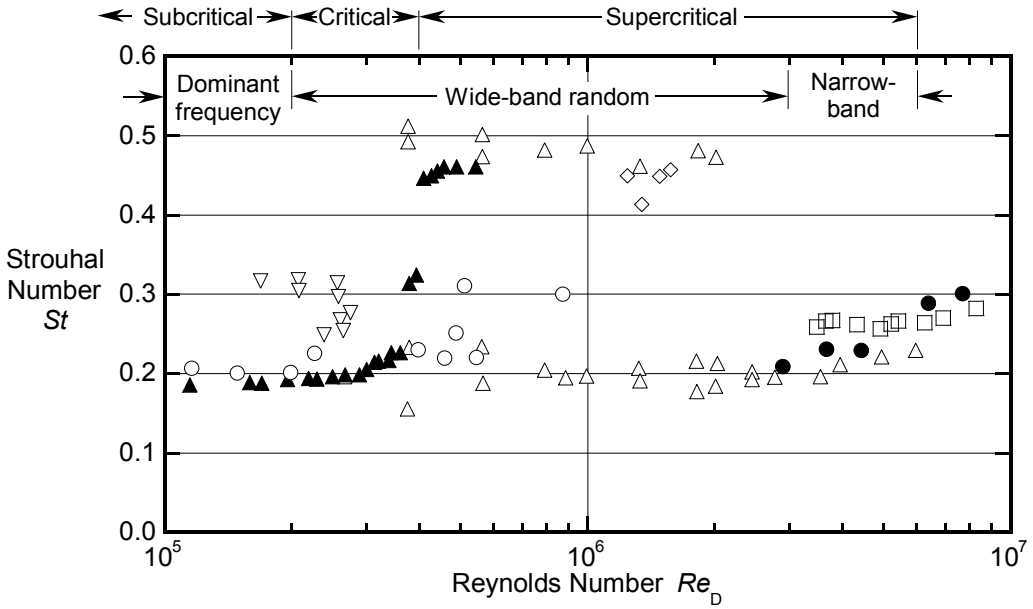

Figure 6. Variation of St with Re for a cylinder in crossflow, as obtained from different investigations, based on figures given by Polhamus (1984).

7.2 Tangent-Ogive Circular Bodies

Modern combat aircraft often operate at high angles of attack throughout their flight manoeuvres, so that the aerodynamic characteristics of their forebodies can significantly influence the flight behaviour of the vehicle. Throughout most of the angle-of-attack range, the flow over the forebodies of such aircraft is significantly influenced by vortical flow, as shown in Figure 7, which is based on a figure given by Chapman & Keener (1979). For low angles of attack, α, the flow remains vortex free over the entire body, provided the flow remains attached to the body. For values of α of 6° to 8°, the crossflow over the body begins to separate at the rear of the body and a pair of symmetrical counter-rotating vortices is formed on the leeward side, as shown in Figure 7a. As α increases, the line of the separating flow moves towards the apex of the body and towards its windward side, and the vortices dominate the flow on the leeward side. For α greater than about 25°, the vortices become asymmetric, as shown in Figure 7b, and when α reaches about 40°, the vortices are asymmetric and are comprised of alternating pairs of vortices, as shown in Figure 7c. For this attitude, significant side forces can be generated, even for bodies having zero sideslip. At higher values of α, an unsteady wake forms behind the body, as shown in Figure 7d.

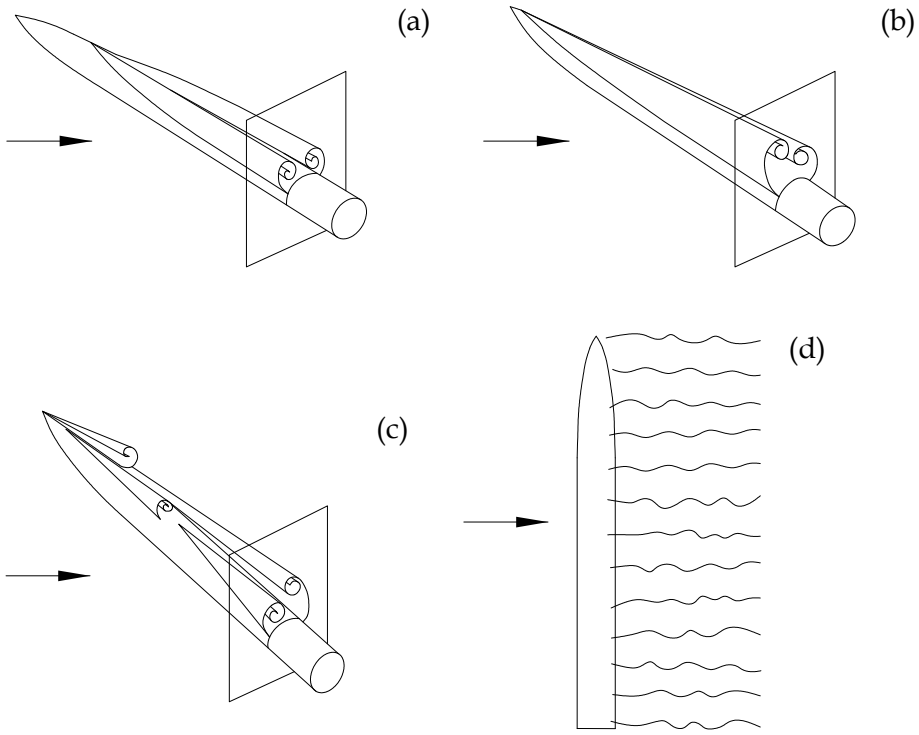

Figure 7. Diagrammatic representation of approximate flow conditions over slender bodies of revolution, based on a figure given by Chapman & Keener (1979).

Figure 8 shows how the normal-force coefficient, C_Z, varies with Reynolds number, Re_D for different values of α for an ogive-cylinder body of revolution for a Mach number, M_t, of 0.5. The circular cylinder has a fineness ratio of 16 and the ogive nose has a fineness ratio of 3. The Reynolds number determines whether the boundary layer on the cylinder is laminar, transitional or turbulent, which in turn strongly influences the flow topology and loads on the cylinder. It can be seen that there is a significant reduction in the critical value of Re_D as α decreases. For a water-tunnel model of a combat aircraft, having a forebody with a diameter of 300 mm, and for the tunnel operating at a free-stream velocity of 0.1 m·s^{-1}, the value of Re_D is about 3×10^4, which is outside the range of the data given in Figure 8. Overall values of C_Z due to forebodies, as measured in water-tunnels, may not be representative of contributions applicable to full-size aircraft.

Figure 9, obtained by Lamont (1982), shows how the maximum side-force coefficient, $C_{Y(max)}$, varies with Reynolds number, Re_D, for different values of α for an ogive-cylinder body of revolution set at $\alpha = 40°$. The circular cylinder has a fineness ratio of 4 and the ogive nose has a fineness ratio of 3.5. As indicated above, when α reaches about 40°, the vortices are asymmetric, and this can produce large side forces, as shown. This can occur even for a symmetrical body set at a zero angle of sideslip. The model was rolled during the experiments to ensure that the maximum side force was measured. Lee *et al.* (2000) indicated that, although the origin of the vortex asymmetry is unclear, it is generally accepted that it is caused by non-uniform surface roughness and/or micro geometrical surface imperfections.

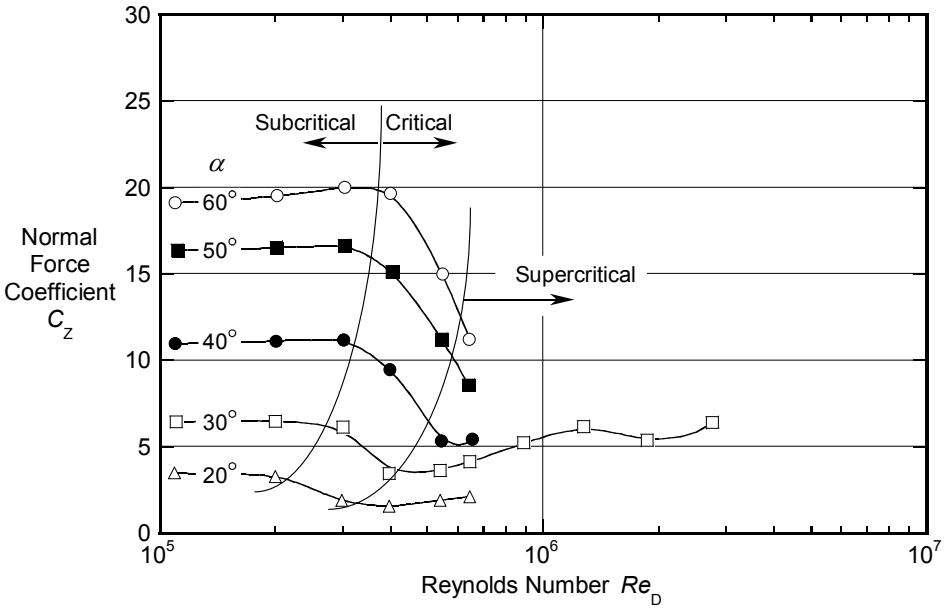

Figure 8. Variation of normal-force coefficient with Reynolds number for different angles of attack for an ogive-cylinder body of revolution for M = 0.5, as obtained by Hartman (1978).

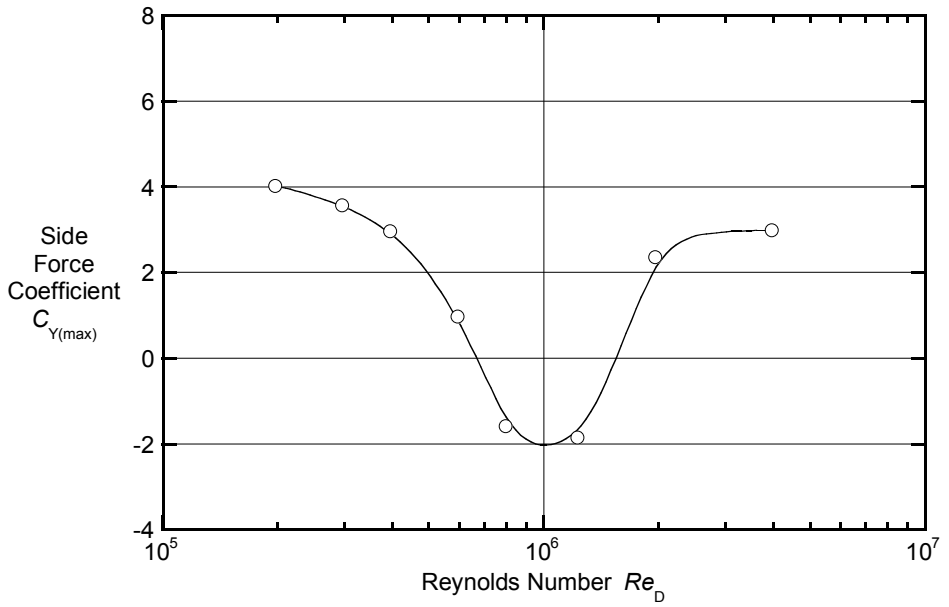

Figure 9. Variation of maximum side-force coefficient with Reynolds number, as obtained by Lamont (1982).

For a water-tunnel model of a circular cylinder, having a diameter of 100 mm and for a free-stream velocity of 0.1 m·s^{-1}, the value of Re_D is about 10^4, which is outside the range of the data given in Figures 5, 6, 8 and 9. The separating flow is strongly dependent on Reynolds number and clearly the water-tunnel data cannot be extrapolated into the critical and supercritical regions.

8. Flow Over Delta Wings

The flow over a delta wing at an angle of attack has been studied extensively by researchers. Side and plan views of the vortical flow over a 70° delta wing at an angle of attack of 30° are shown in Figures 10a, b –see Erm, 2003. The nominal free-stream velocity in the test section of the tunnel was 0.1 $m \cdot s^{-1}$, giving a Reynolds number of about 3.0×10^4 (based on the centreline chord of the wing, c = 300.0 mm). The flow is dominated by two large bound counter-rotating vortices that are formed by the rolling up of the flow that separates along the two leading edges of the wing. These vortices produce intense suction peaks on the wing surface under their cores and this contributes significantly to the lift on the wing. As α increases, the pressure on the leeward side of the wing decreases and the cores of the vortices can become unstable and they break down or burst. The breakdown is characterised by a sudden expansion in the size of the vortex core, a rapid deceleration of the axial velocity in the core, a steep increase in the pressure and an increase in the turbulence downstream of the breakdown region. As α increases, the breakdown region moves towards the apex of the wing.

A technique has been developed at DSTO to measure the very small flow-induced pressures on the surface of a model in a water tunnel –see Erm, 2003. Pressures were measured on the delta wing for different flow conditions. Pressure coefficients, shown in Figure 10c, were measured at different values of y/s for values of x/c of 0.3, 0.4, 0.5, 0.6 and 0.8, where y is the spanwise distance from the centreline chord of the wing, s is the local semi-span of the wing and x is the chordwise distance from the apex of the wing. Grids showing values of x/c and y/s have been superimposed on the images of the vortical flow, enabling the C_p distributions to be correlated directly with the images.

For each C_p distribution given in Figure 10c, values of C_p are least negative at the centreline chord of the wing and are most negative on the regions of the wing under the cores of the vortices, i.e. suction peaks exist under the vortices. The regions where values of C_p are most negative correspond closely to $y/s = \pm 0.6$.

In Figure 11, the DSTO C_p measurements taken on the 70° delta wing in the water tunnel are compared with similar measurements taken by McKernan (1983) ($Re = 2.25 \times 10^5$), Roos & Kegelman (1990) ($Re = 4.0 \times 10^5$) and Atashbaz & Ahmed (1997) ($Re = 4.8 \times 10^5$), for $x/c = 0.75$ and $\alpha = 30°$, on 70° delta wings in wind tunnels. It was necessary to use interpolated data in most cases to make the comparison. The C_p distributions on the delta wing in the water tunnel have the same general characteristics and trends as similar measurements given by the other researchers. There is generally good agreement between the DSTO water-tunnel data and the wind-tunnel data. Differences do occur in the region under the vortex core, but considering the differences in Reynolds numbers and the fact that the data are in the post-breakdown condition, these differences in peak suction values are not surprising. The good agreement suggests that the technique used to measure the low flow-induced pressures in the water tunnel is viable.

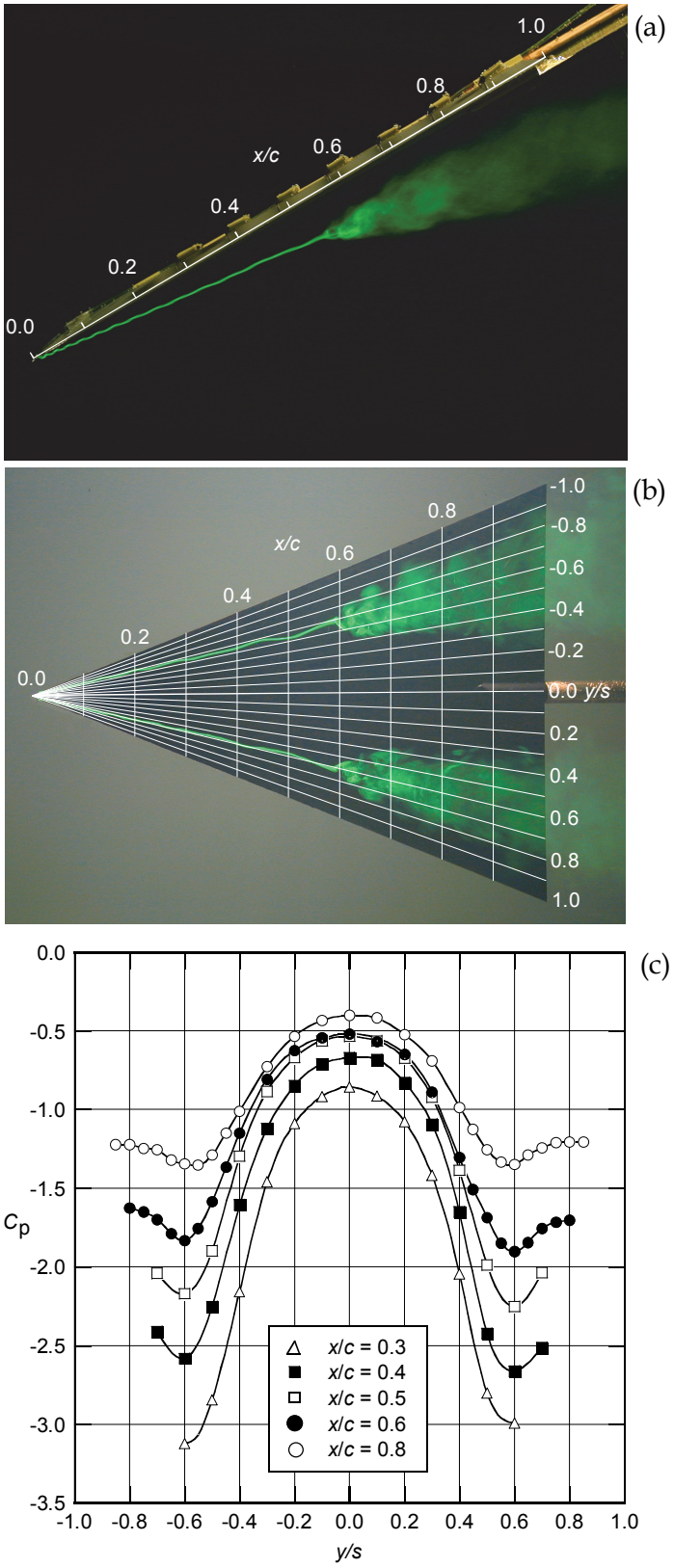

Figure 10. Characteristics of the flow over a 70° delta wing for $\alpha = 30°$. (a) side-view image, (b) plan-view image, (c) pressure coefficients.

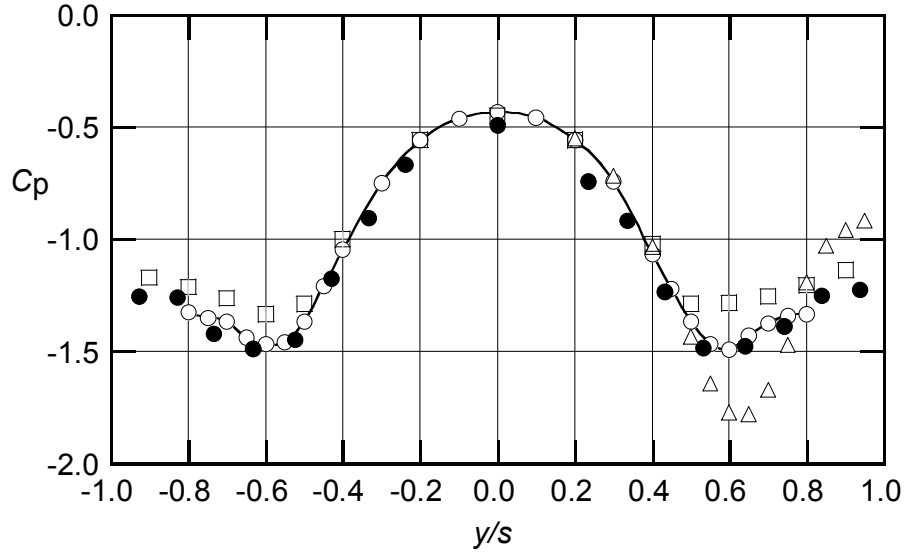

Figure 11. Comparison between pressure coefficients measured on a delta wing in the DSTO water tunnel and in wind tunnels for x/c = 0.75 and $\alpha = 30°$. ○ DSTO water-tunnel; □ McKernan (1983); ▵ Roos & Kegelman (1990); ● Atashbaz & Ahmed (1997).

Figure 12 shows the location of vortex breakdown *vs* α for 70° delta wings, as obtained by different researchers using a wide range of facilities. Reynolds numbers vary from about 1.7×10^4 to about 1.6×10^6. The variation in the data for the different investigations is substantial, predominantly at the lower values of α, and there does not appear to be any trend with Reynolds number. The water-tunnel data of Miau *et al*. (1992) and Kowal & Valiki (1998) lie within the bounds of the wind-tunnel data. Sharp-edge bodies are known to exhibit remarkable Reynolds-number independence, so most likely the variations between the different data sets are due to differences in tunnel blockage, support interference, leading edge on the delta wings (blunt, single bevel, double bevel, different bevel angles), uniformity of the flow, tunnel free-stream turbulence level, model centrebody, aeroelastic behaviour of a model, and model support sting.

Figure 13 shows how C_Z varies with α for 70° delta wings, as obtained by researchers using a wide range of facilities, as well as from CFD studies. Reynolds numbers vary from about 4×10^4 to about 2×10^6. Values of C_Z from the different investigations collapse reasonably well at the lower values of α, but there is significant variation at the higher values of α. Once again, there does not appear to be any trend with Reynolds number. Possible reasons for discrepancies between the different data sets are the same as those given above for the variation in the position of the breakdown region. Although the variation in the flow topology is substantial, as depicted by the large variation in breakdown locations with α (Figure 12), this is not reflected in the variation of the global loads on the wings (Figure 13).

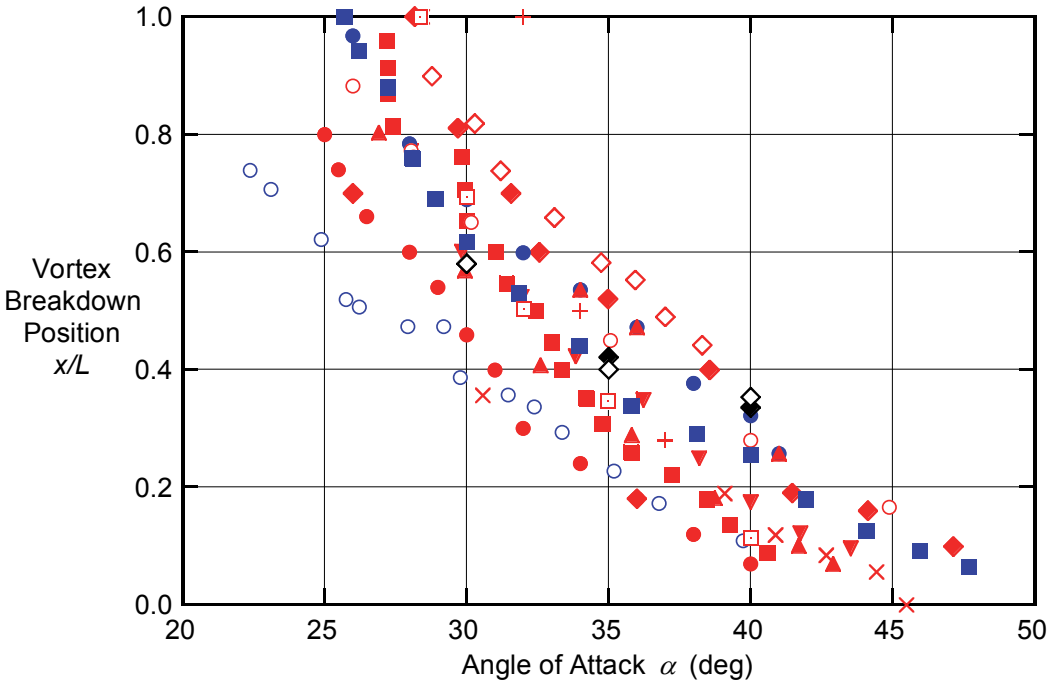

Symbol	Researchers	Facility	Reynolds Number
○	Kowal & Valiki (1998)	Water Tunnel	1.70 x 10^4
●	Miau *et al.* (1992)	Water Tunnel	1.70 x 10^4
◆	Traub *et al.* (1998)	Wind Tunnel	4.00 x 10^4
■	Erikson (1981)	Water Tunnel	4.10 x 10^4
○	McKernan & Nelson (1983)	Wind Tunnel	1.13 x 10^5
◇	Le May *et al.* (1990)	Wind Tunnel	2.60 x 10^5
■	Roos & Kegelman (1994)	Wind Tunnel	4.00 x 10^5
▼	Payne (1987)	Wind Tunnel	4.25 x 10^5
□	Elle (1961)	Wind Tunnel	6.50 x 10^5
+	Lawford & Beauchamp (1963)	Wind Tunnel	1.05 x 10^6
▲	Lowsan & Riley (1994)	Wind Tunnel	1.145 x 10^6
X	Kohlman &Wentz (1971)	Wind Tunnel	1.145 x 10^6
●	Mitchell *et al.* (1998)	Wind Tunnel	1.57 x 10^6
◆	Goertz (2002)	CFD Lam NS	1.97 x 10^6
◇	Goertz (2002)	CFD Euler	

Figure 12. Variation of vortex breakdown position with α for 70° delta wings for different investigations, based on a figure given by Munro et al. (2005). (Blue symbols are used for water-tunnel data, red symbols for wind-tunnel data, black symbols for CFD studies). (The legend is arranged in order of increasing Reynolds number).

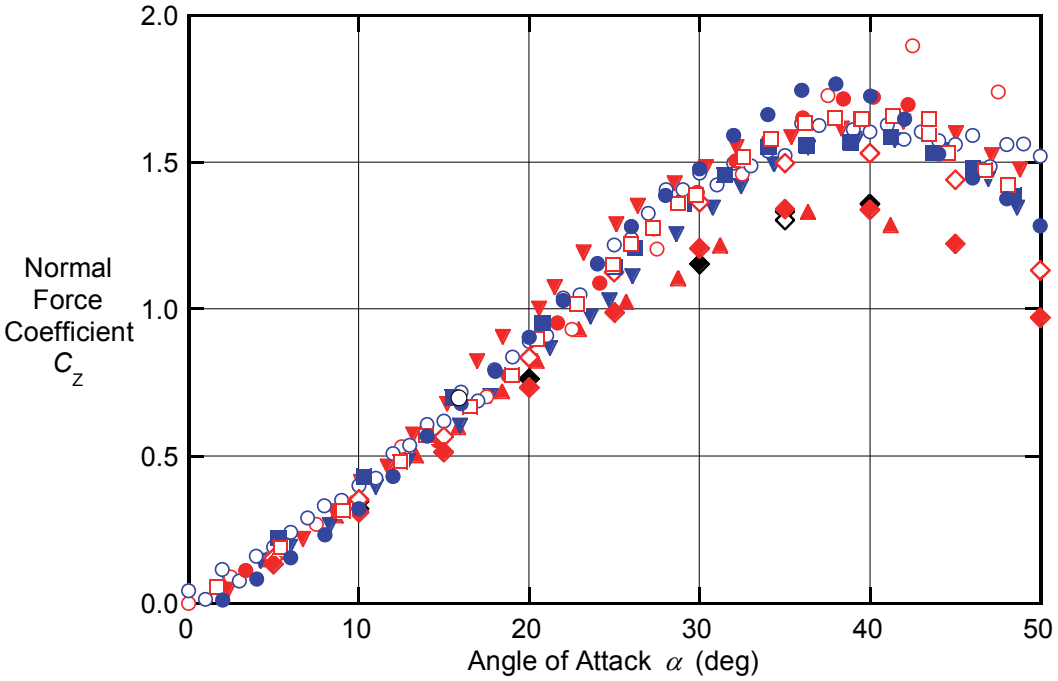

Symbol	Researchers	Facility	Reynolds Number
●	Erm (2006a)	Water Tunnel	2.00 x 10^4
■	Suarez *et al.* (1994)	Water Tunnel	3.90 x 10^4
O	Munro *et al.* (2003)	Water Tunnel	5.51 x 10^4
▼	Cunningham & Bushlow (1990)	Water Tunnel	6.60 x 10^4
▲	Brandon & Shah (1990)	Wind Tunnel	4.00 x 10^5
O	Earnshaw & Lawford (1966)	Wind Tunnel	4.53 x 10^5
▼	Jarrah (1989)	Wind Tunnel	8.50 x 10^5
●	Phillis (1991)	Wind Tunnel	1.00 x 10^6
◇	Soltani, Bragg & Brandon (1988)	Wind Tunnel	1.00 x 10^6
□	Wentz & Kohlman (1968)	Wind Tunnel	1.10 x 10^6
◆	Rizzi, Goertz & Munukka (1999)	CFD Lam BL	1.97 x 10^6
◇	Rizzi, Goertz & Munukka (1999)	CFD Turb BL	1.97 x 10^6
◆	Soltani, Bragg & Brandon (1988)	Wind Tunnel	1.97 x 10^6

Figure 13. C_Z vs α for 70 °delta wings for different investigations, based on a figure given by Munro et al. (2003). (Blue symbols are used for water-tunnel data, red symbols for wind-tunnel data, black symbols for CFD studies). (The legend is arranged in order of increasing Reynolds number).

9. Flow Over an F/A-18 Aircraft

Wind- and water-tunnel tests as well as full-scale flight trials have been undertaken by different researchers using an F/A-18 configuration to determine the breakdown position of the vortex emanating from the leading-edge extension (LEX) for different angles of attack. Images of the vortical flow over a 1/48 size model of an F/A-18 aircraft for an angle of attack of 23°, as obtained in the DSTO water tunnel, are shown in Figure 14. The variation of the breakdown location with angle of attack, as determined by different investigators, is shown in Figure 15. Despite the fact that Reynolds number and Mach number were not simulated in the tunnel tests, the locations of vortex breakdown for the tunnel data are approximately the same as for the flight-test data. This contrasts to the high variability of the location of vortex breakdown with angle of attack displayed by delta wings, as shown in Figure 12. Possible reasons for the insensitivity of the breakdown region to the angle of attack for the F/A-18 configuration are given below.

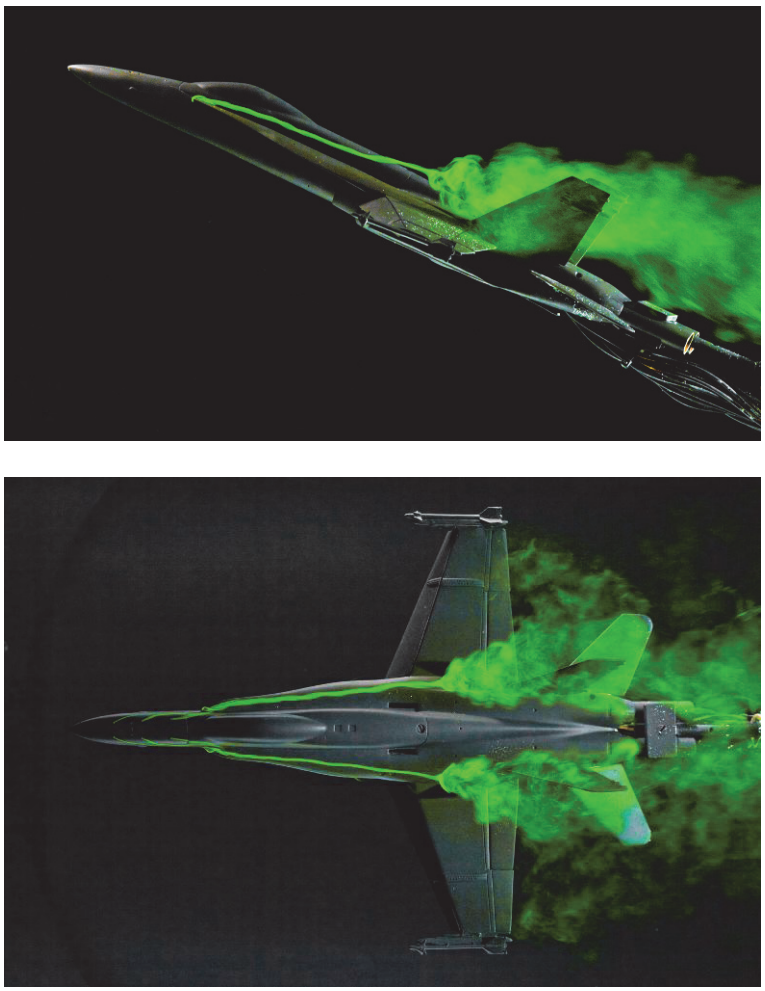

Figure 14. Side- and plan-view images of vortical flow over a 1/48 size model of an F/A-18 aircraft for $\alpha = 23°$, as obtained in the DSTO water tunnel.

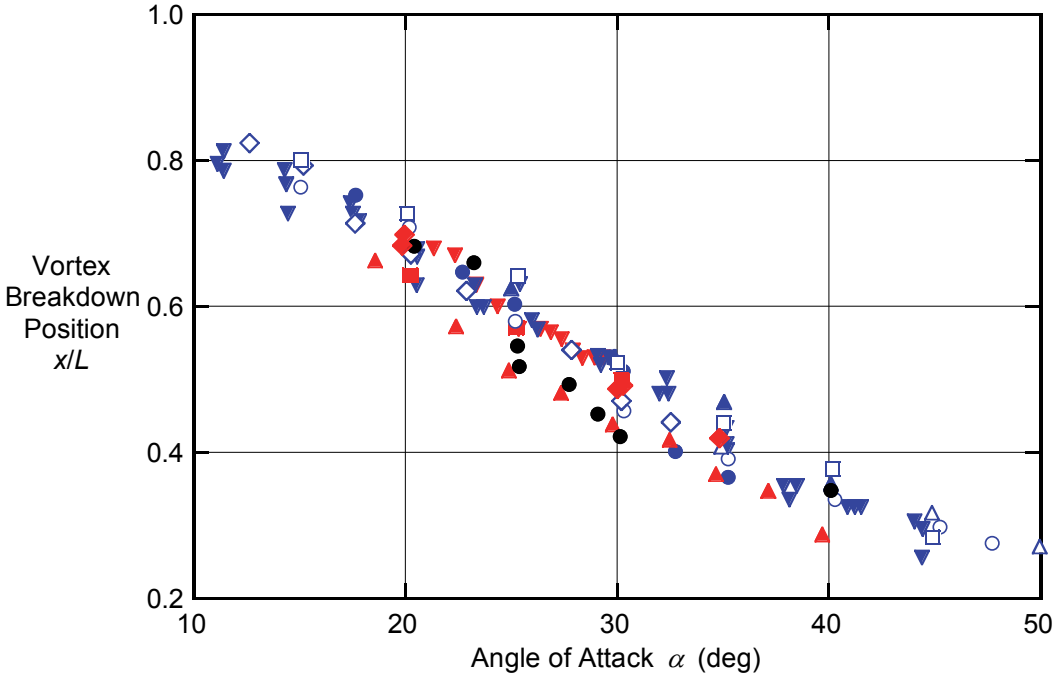

Symbol	Establishment	Facility	Reynolds Number
●	NAE	Water Tunnel	5.00 x 10^3
▼	DSTO (Thompson, 1990)	Water Tunnel	5.12 x 10^3
O	IAR	Water Tunnel	6.50 x 10^3
△	IAR OPLEC	Water Tunnel	6.50 x 10^3
▲	Dryden FVF unmodified	Water Tunnel	8.10 x 10^3
□	Dryden FVF modified	Water Tunnel	8.10 x 10^3
◇	Dryden	Water Tunnel	1.26 x 10^4
▼	DSTO (Thompson, 1990)	Wind Tunnel	1.34 x 10^5
◆	BART	Wind Tunnel	1.60 x 10^5
■	McAir	Wind Tunnel	3.60 x 10^5
▲	DTRC	Wind Tunnel	1.75 x 10^6
●	Dryden	Flight	8-13 x 10^6

Figure 15. Variation of vortex breakdown position with α for an F/A-18 configuration for different investigations, based on a figure given by Beyers & Ericsson (2001). (blue symbols are used for water-tunnel data, red symbols for wind-tunnel data, black symbols for CFD studies). (The legend is arranged in order of increasing Reynolds number).

Figure 16 shows values of C_Z *vs* α, as measured on models of F/A-18 aircraft in wind and water tunnels. The wind- and water-tunnel data show good agreement, despite the significant

variations in test Reynolds and Mach numbers, due to the similar vortical flow patterns over the aircraft for the different cases.

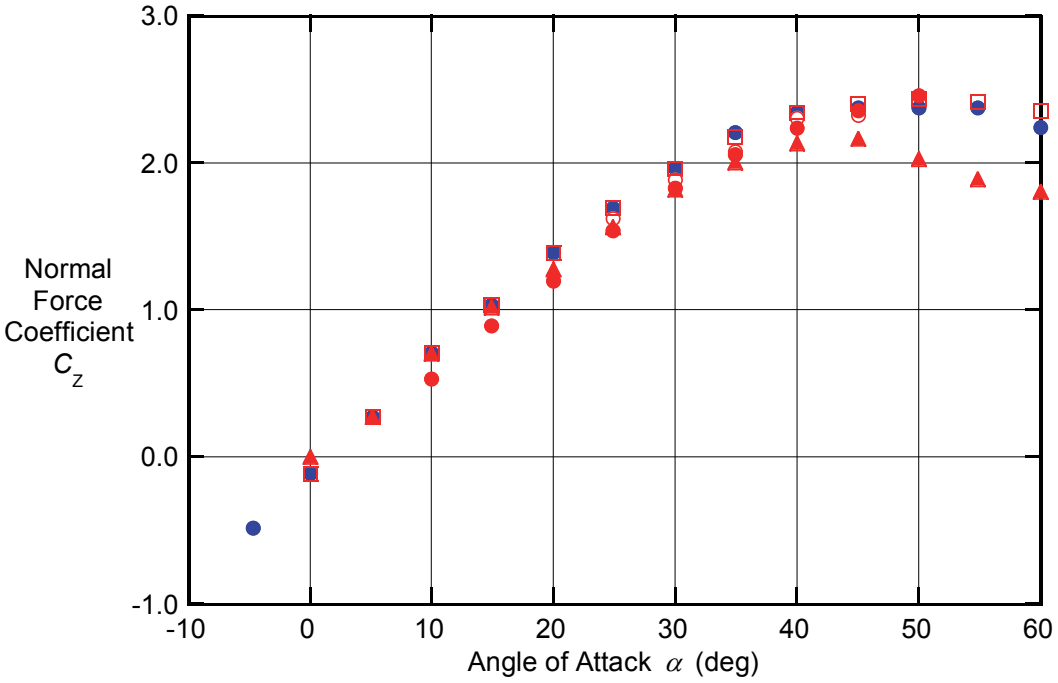

Symbol	Researchers	Facility	Reynolds Number
●	Suarez & Malcolm (1994)	Water Tunnel	1.25×10^4
▲	Brandon & Shah (1999)	Wind Tunnel	2.70×10^5
□	Kramer *et al.* (1993)	Wind Tunnel	6.50×10^5
●	Erickson *et al.* (1989)	Wind Tunnel	1.20×10^6
O	Lanser & Murri (1993)	Wind Tunnel	Full Scale

Figure 16. C_Z vs α for an F/A-18 configuration for different investigations, based on a figure given by Suarez & Malcolm (1994). (blue symbols are used for water-tunnel data, red symbols for wind-tunnel data). (The legend is arranged in order of increasing Reynolds number).

Modern combat aircraft have shapes that are basically comprised of a slender circular forebody with a pointed nose and a sharp-edged delta wing. As discussed in previous sections, data acquired in water tunnels for models with rounded leading edges do not scale well to full-size vehicles, due to different types of flow separation for the two cases. Data for delta-wing models are most likely not affected significantly by variations in Reynolds-numbers. Consequently incremental loads measured on the forebodies of aircraft models in water tunnels will not be representative of those for full-size vehicles and this will affect the overall accuracy of scaled loads.

Despite the above finding, it has been shown that flow patterns and normal-force coefficients acquired using a model of an F/A-18 aircraft in water tunnels agree well with data for a full-

size F/A-18. Beyers & Ericsson (2001) addressed this issue and found that the insensitivity of the breakdown region to the angle of attack for the F/A-18 configuration was due in equal parts to the Gothic apex geometry of the LEX planform and "viscous fairing" effects on the fuselage-induced upwash at the LEX leading edge downstream of the apex. Additionally, an effective sweep angle increase, induced by the viscous-fairing effects, tends to compensate for the lack of a compressibility effect in water tunnels. Whether this fortuitous situation applies to other aircraft is a matter of conjecture.

10. Dynamic Testing in Water Tunnels

"Dynamic testing" is a broad and amorphous term, connoting motion of a test article with respect to a laboratory frame of reference. A detailed list of dynamic-testing subtopics may be:

1. Standard measurement of dynamic-stability derivatives for relatively conventional airplanes in assumed linear conditions. These are typically the roll, pitch and yaw damping derivatives, measured by forced sinusoidal oscillation about a trim point. The application would be building the flight-dynamic model and control laws.
2. Spin-tests and other forced or free oscillations, where the objective is to assess departure-characteristics of the airplane, presumably in conditions peripheral to the normal performance envelope, but important for safety certification.
3. High-alpha/high-rate tests, where one is interested in helicopter blade dynamic stall, or maneuvers for aerobatic/combat aircraft. Large flow separations and concomitant nonlinearities are expected. Here one is interested in both the 6 degree-of-freedom aerodynamic loads and flow-field measurements to elucidate the causes behind those loads. This area also includes (a) leading-edge vortices of sharp-edged highly-swept configurations, and (b) the vortical structures emanating from missiles, forebodies and after-bodies at high angles of attack.
4. Aeroelastic tests, where an intentionally flexible model undergoes measurable time-dependent deflections, and may be tested to destruction, to ascertain flutter limits and other fluid-structure interaction problems. Problems include safeguarding the tunnel from damage by model debris, and time-resolved measurements of structure and flowfield.
5. Micro Air Vehicles (MAVs) and related small Uninhabited Air Vehicles (UAVs), which are capable of violent manoeuvres and are expected to encounter strong wind gusts, relative to their flight speed. This includes flapping-wing MAVs, which always operate in an unsteady flowfield. For this application there is little distinction between basic research and engineering testing.
6. Store-separation tests, such as with a captive-trajectory system, involving relative motion of two or more bodies. Typical problems are at high flight speeds, involving compressibility.
7. Wind-engineering tests, including fixed ground structures, ground-vehicles, aircraft in landing scenarios, etc., where a high-turbulence environment is simulated together with ground-effect.

8. Gust tests, where the tunnel is shuttered or otherwise the free-stream is modified from steady, to assess aircraft response to transient flowfield conditions.
9. Free-flight tests, where the aircraft is tethered or completely free, and is "flown" in the tunnel test section, thus combining testing of aerodynamics and flight dynamics.

The advantage of water tunnels in dynamic testing is that for a given reduced frequency of motion (scaled by model length scale and tunnel free-stream velocity) the physical rate of motion is much smaller in water than in air. This makes data acquisition much easier. Dynamic tares to remove the model inertial forces, are either very easy or sometimes completely unnecessary, in contradistinction to wind-tunnel testing, where dynamic tares are difficult and the inertial load dominates the total measured load, –see Kramer (2002). Flow visualization is made easier by the slower physical rates of motion. Mechanism design and model construction are much easier, since models can be heavier and internal loads in the forced-oscillation rig will be much lower.

However, some dynamic tests are either impossible or very difficult in water. Item 6 is beyond the scope of water tunnels whenever compressibility is important, such as in cavity acoustics. Item 9 is not amenable to water tunnels because of the tunnels' small size, and because of the difficulty of propelling a "flight" article in water (the exception is flapping-wing MAVs). Froude scaling, necessary for free-flight tests, becomes problematic because of the density of water. Item 2 is in principle possible, but again is awkward because of water tunnels' small size and Froude scaling. This is best done in an open-jet wind tunnel.

Aeroelastic scaling, Item 4, is both problematic and promising in water tunnels. It is problematic because it is impossible to match the density ratio between the model material and water. Any test requiring high model surface fidelity is unlikely to be successful, for the same reasons as for static problems. And the aforementioned problems with force balances also hold for dynamic tests, though again the low motion rates in water offer much advantage. However, the mechanics of aeroelastic testing in water are easier because broken models are easily contained before parts go downstream to potentially damage the pump –a huge concern in wind-tunnel testing. And the slow rates make recording of model vibration easier.

Item 7 is usually reserved for large wind tunnels, owing to a need for proper separation of lengths scales of the desired ambient turbulence environment, and the need for relatively large models with fine structure. The chief obstacle in running such tests in water tunnels is the difficulty in obtaining the "right" turbulence environment. This raises the larger question, of how does one characterize water-tunnel-test-section flow quality. It is not a trivial topic, since hot wires and Pitot tubes perform marginally in water, requiring alternative or at least improved techniques.

Shuttering a wind tunnel, Item 8, is a convenient means of producing well-defined gusts –see Williams *et al*. (2008), for gust-response testing, and for producing disturbances in general, for system-identification tests. Shuttering a water tunnel is difficult because of the density of water, the resulting pressures (water hammer), and risk of spillage. However, for the same reason that high-rate testing in water tunnels is straightforward, impulsive-start testing, such as to validate classical models such as Wagner's, is readily possible in water tunnels, but very difficult in wind tunnels. One example is use of a piston-driven water tunnel, producing very

rapid acceleration of the free-stream, for studying impulsive-start problems for airfoils at high angles of attack, –see Soria, *et al*. 2003. Such an experiment is impossible in wind tunnels. For water tunnels with a long test section, such as the US AFRL water tunnel, it is possible to run the tunnel as a tow tank, with the model carriage translated on rails in the free-stream direction, modelling a "gust" by moving the model, or modelling impulsive-start by violent acceleration. It should in principle be possible to run close approximations to indicial motions, thus explicitly constructing the indicial response integral –see Etkin (2005), opening new vistas in massively-unsteady aerodynamics. But this is a niche area, of interest at present primarily to just MAVs.

Item 1 is the main-line dynamic test in aeronautical engineering. Its outlook for swept-wing configurations in water tunnels is discussed by Kramer (2002), who points out remarkable similarity in dynamic-derivative data between water tunnels, wind tunnels and flight test, but also notes the ease of obtaining such data in water tunnels. It remains however to systematically assess the outlook for low-sweep configurations lacking sharp leading edges, such as transport aircraft. Again the crux of the problem is Reynolds-number scaling. The authors would like to refrain from definitive recommendations, pending a systematic comparison between wind-tunnel and water-tunnel tests on a common configuration.

Water tunnels perform brilliantly for Items 3 and 5: for high-rate testing, especially for MAVs, where it is essentially impossible to produce the requisite motion dynamics in air, but straightforward to do so in water. Here we consider an example, from the US Air Force Research Laboratory, Air Vehicles Directorate water tunnel. The test case is sinusoidal pure-plunge of a Selig SD7003 airfoil, and Reynolds number 4×10^4 based on airfoil chord and free-stream flow speed (~26 cm·s^{-1}). The reduced frequency is the very high value of 3.93, but the physical frequency is only 0.54 Hz! The reduced amplitude of plunge oscillation is 0.05. Because the motion is periodic, we are interested in phase-averages of the flowfield response. In Figure 17, the top row of vorticity contours is taken at the phase of motion corresponding to the top of the plunge stroke; the second row is at halfway down the plunge stroke, where motion-induced angle of attack is maximum positive; the third row is at the bottom of the plunge stroke; and the fourth and final row is at halfway back up the plunge stroke, where motion-induced angle of attack is maximum negative. Experiment (PIV) is compared with two different computations. Apart from dissipative effects in the computation, the mutual comparison is striking. This sort of experiment is crucial for flapping-wing MAVs –and essentially impossible in wind tunnels, where the required high physical frequency of motion would likely destroy the motion rig, or at least make the data acquisition very problematic.

As MAV applications emerge from a niche area into more regular aeronautical engineering practice, the relevance and importance of water tunnels promises to increase. The one word of caution is regarding aeroelastic scaling; most MAV configurations are structurally flexible, and structural scaling in water can be problematic. Rigid abstract shapes –airfoils, plates and the like, undergoing high-rate motions– are easiest to test in water tunnels. Full configurations are harder –which is precisely the same scenario as for static testing.

A water-tunnel dynamic-testing system has been developed at DSTO by Erm (2006b) that enables instantaneous flow-induced forces and moments on a model to be measured while it is in motion undergoing a predetermined dynamic manoeuvre in roll, pitch and yaw. Using the system, it is possible to measure static and dynamic aerodynamic derivatives for the

model for a specified motion. Dedicated software has been written to enable to system to be controlled via a PC using a graphical user interface.

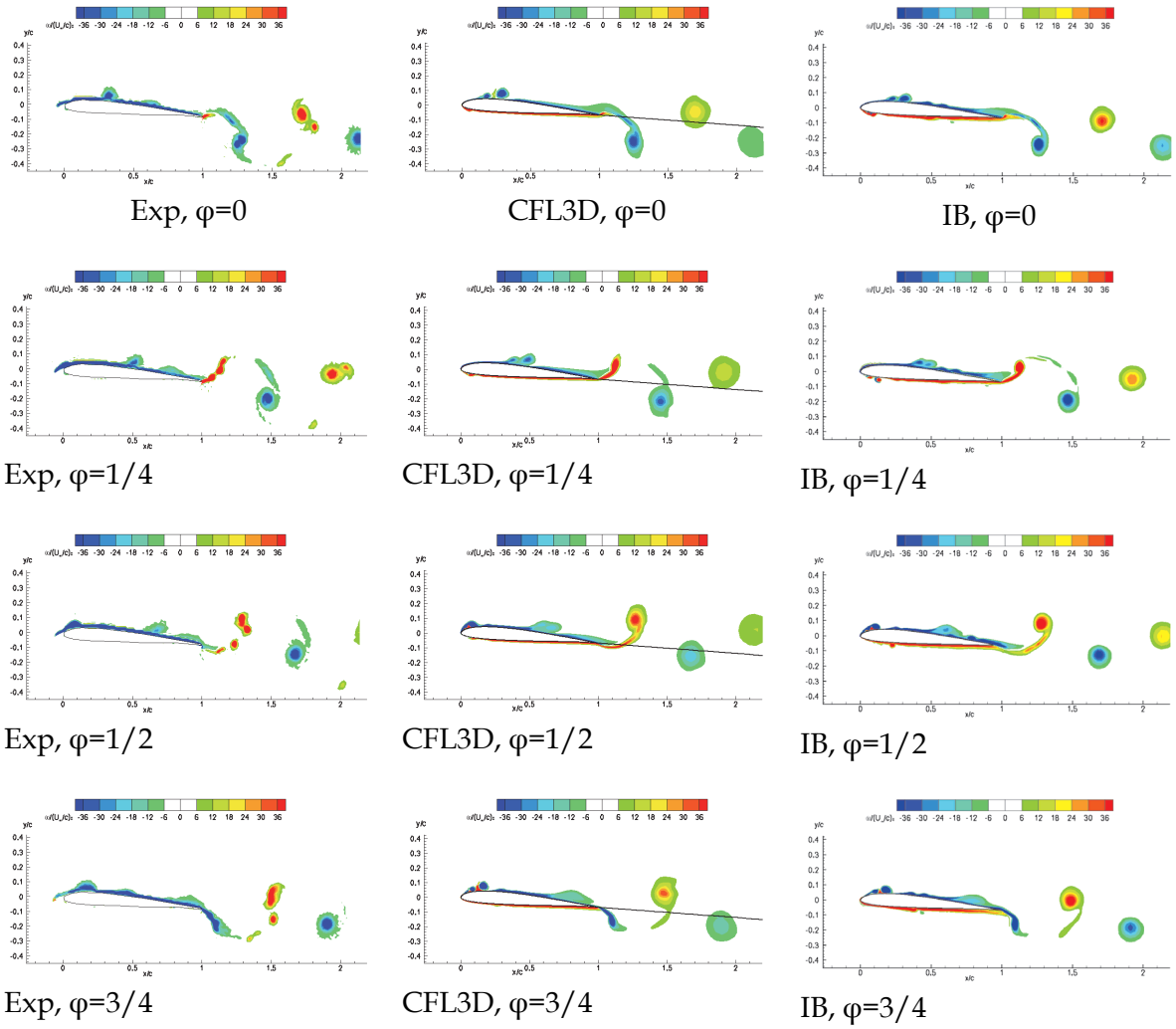

Figure 17. Comparison of out-of-plane vorticity contours from experiments in the water tunnel (left column), 2D computations using the commercial code CFL3D, and 2D immersed boundary-method computations, at various phases of motion; Re = 4 × 10⁴, SD7003 airfoil pure-plunge.

Tests have been carried out by Erm (2011) in the DSTO water tunnel using a Standard Dynamics Model (SDM), shown in Figure 18, to measure longitudinal force and moment coefficients as well as longitudinal static and dynamic aerodynamic derivatives. Data were processed using the methodology developed by Newman (2011). Selected data from the water-tunnel investigation are reproduced below. Values of C_Z, C_m and $C_{mq} + C_{m\dot{\alpha}}$ measured in the water tunnel are shown in Figures 19, 20, and 21 respectively using red symbols, where C_Z and C_m are the normal-force and pitching-moment coefficients respectively, and $C_{mq} + C_{m\dot{\alpha}}$ is a combined dynamic derivative for the pitching moment, due to the effects of pitch rate and angle of attack rate. Values of C_Z and C_m were measured with the SDM stationary at different pitch angles, θ, and values of $C_{mq} + C_{m\dot{\alpha}}$ were measured with the SDM oscillating by ±0.5° in pitch with simple harmonic motion about different mean values of θ. Corresponding data

acquired by other researchers using wind tunnels are superimposed on the DSTO data in Figures 19 to 21 using black symbols. Details of the wind-tunnel investigations are given in Table 4.

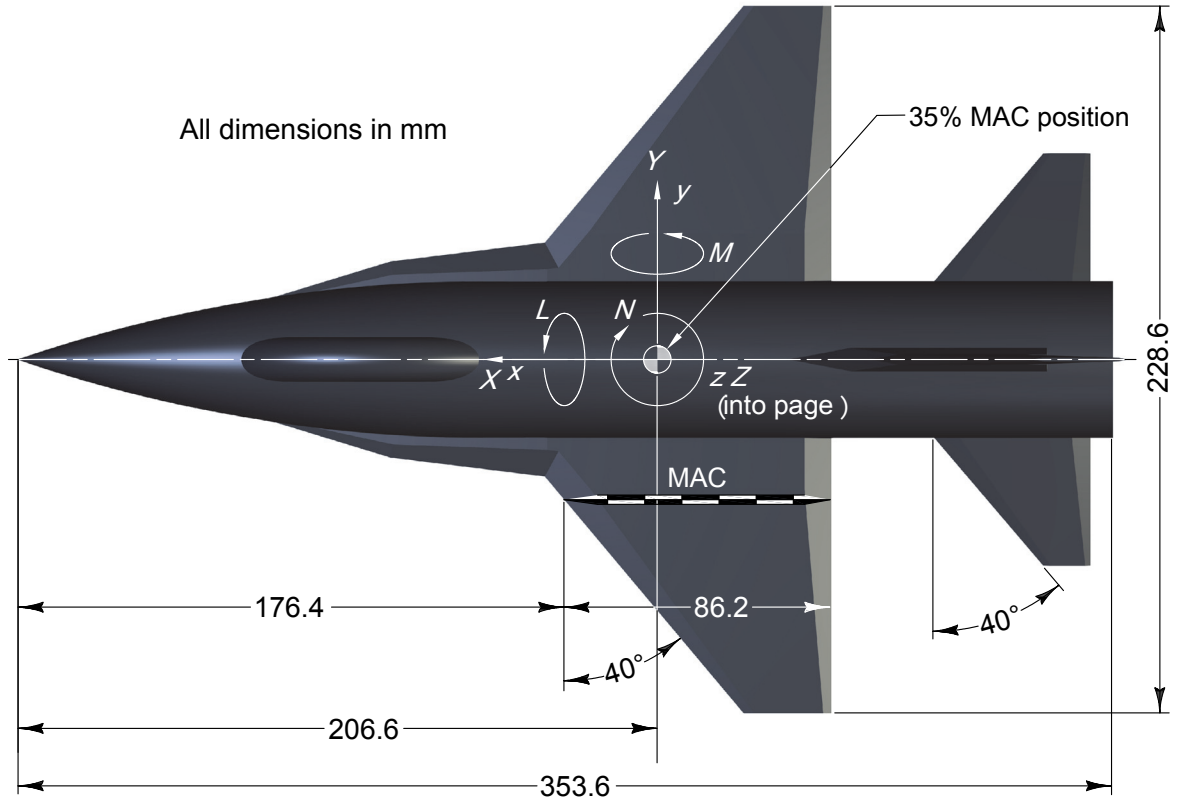

Figure 18. Details of the SDM used in DSTO water tunnel.

Although many researchers have carried out tests in wind tunnels using SDMs to measure static and dynamic derivatives, there is not a standardised testing schedule. SDMs of different sizes have been tested, having spans varying from 228.6 mm to 701.4 mm. Tunnel operating conditions have varied from high-velocity flows, having Mach numbers of 0.6 and beyond, down to low-velocity flows of 30 $m \cdot s^{-1}$ or less. Reduced frequencies of oscillation and oscillation amplitudes have also varied. Each tunnel had its own unique dynamic-rig configuration, used to oscillate a SDM. These rigs were often substantial, resulting in significant tunnel blockages, which varied from tunnel to tunnel, affecting the quality of the flow around a SDM in different ways. All of the above differences in the testing programs inevitably lead to variations in acquired data for the different cases. The tests are highly specialised and there is no definitive data set to be used for comparison purposes. Despite the above reservations, and although there are variations in acquired data from the different investigations, general trends can be discerned.

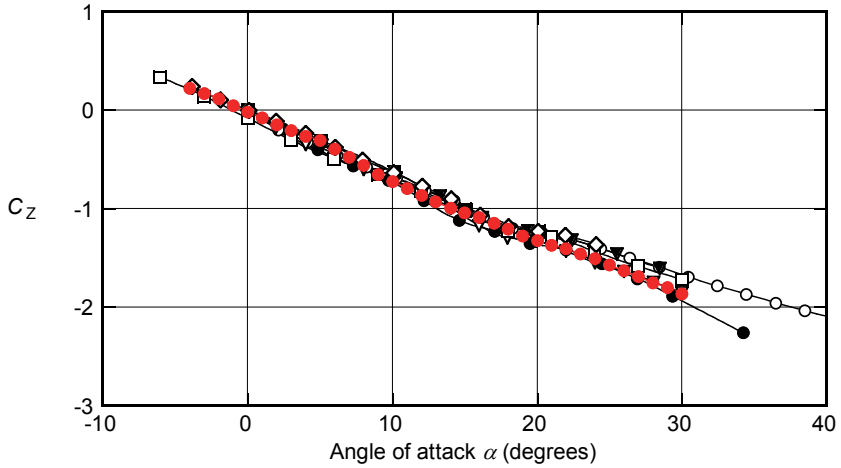

Figure 19. C_Z vs α for SDMs for different investigations – see legend below.

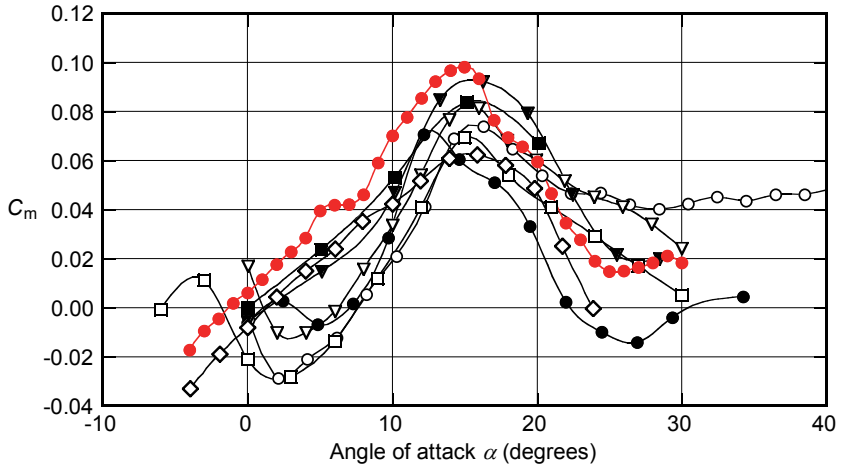

Figure 20. C_m vs α for SDMs for different investigations – see legend below.

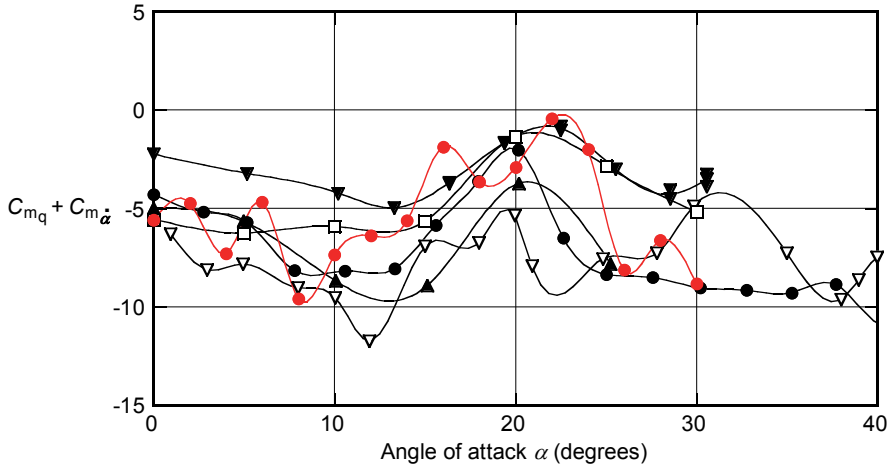

Figure 21. $C_{mq} + C_{m\dot{\alpha}}$ vs α for SDMs for different investigations.

Legend for Figures 19 to 21: ◇ Cyran (1981), M_t = 0.6; ● Beyers *et al*. (1984) (also see Beyers 1985), M_t = 0.6; ▼ Schmidt (1985), M_t = 0.6; ○ Huang & Beyers (1990), V = 70 m·s^{-1}; ▽ Guglieri & Quagliotti (1991), M_t = 0.1 to 0.2; ▲ Kabin *et al*. (1995), M_t = 0.6; ■ Ueno & Miwa (2001), M_t = 0.6; □ Alemdaroglu *et al*. (2001), V = 30 or 40 m·s^{-1}; ● Erm (2011) (DSTO water tunnel), V = 0.1 m·s^{-1}.

Values of C_Z, C_m and $C_{m_q} + C_{m_{\dot{\alpha}}}$ measured in the water tunnel, shown in Figures 19, 20 and 21 respectively, are as acceptable, i.e. no better or no worse, than wind-tunnel data. This was also found this to be the case for other SDM derivatives. Although the C_m data lie outside the general scatter of the wind-tunnel data for $\alpha < 15°$, the discrepancy between the water-tunnel data and adjacent wind-tunnel data is less than the overall scatter of the wind-tunnel data. The above suggests that it is feasible to use a water tunnel to measure load coefficients and derivatives on an aircraft model in a water tunnel, at least for the SDM geometry.

Table 4. Summary of experimental investigations undertaken by different researchers in different facilities using a Standard Dynamics Model.

Researchers Establishment	**SDM Span (Scale)***	**Velocity Reynolds Number Mach Number**
Cyran (1981) AEDC (USA)	502.9 mm (2.2)	Re/ft = 0.5 × 10⁶ to 5.0 × 10⁶ M_t = 0.3 to 1.3
Beyers *et al*. (1984) also see Beyers (1985) NAE (Canada)	228.6 mm (1.000)	Re/m = 10.4 × 10⁶ M_t = 0.6
Schmidt (1985) DFVLR (Germany)	344.89 mm (1.509)	Re = 1.03 × 10⁶ to 1.54 × 10⁶ M_t = 0.60 to 1.20
Huang & Beyers (1990) NAE (Canada)	228.6 mm (1.000)	V = 69 , 100 m·s^{-1} Re = 3.9 × 10⁵, 5.7 × 10⁵
Guglieri & Quagliotti (1991) TPI/TU (Italy)	609 mm (2.664)	Re = 4.0 × 10⁵, 6.6 × 10⁵ $M_t \approx 0.1$
Kabin *et al*. (1995) Russia	360 mm (1.575)	M_t = 0.60
Ueno & Miwa (2001) (NAL) Japan	701.4 mm (3.068)	Re = 2.31 × 10⁶ to 2.95 × 10⁶ M_t = 0.6 to 1.05
Alemdaroglu *et al*. (2001) Middle East Technical University (Turkey)	609 mm (2.664)	V = 20 , 30 , 40 m·s^{-1}
Erm (2011) DSTO (Australia)	228.6 mm (1.000)	V = 0.1 m·s^{-1}

* (Scale relative to DSTO SDM).

11. Rapid Prototyping of Water-Tunnel Models

The cost and time savings of water tunnels can only be realized if every test component is inexpensive, including the model. Wood or aluminium models are common in small wind tunnels, but create problems in water due to absorption of water, oxidation, and deterioration of surface finish. Of course, these are no great problem for short tests (< 1 day of total immersion time). The alternative –stainless steel– is expensive to machine. A better alternative is rapid prototyping of plastic models. As of this writing, for about $200k USD one can obtain a "3D printer" capable of 0.0006 inch build-layer (0.015 mm), in a build volume of 12 inch cubed. Assuming a good three-dimensional input file, the cost per model is <<$1000 USD, and involving perhaps one man-day of setup and post-finishing. And a "good" 3D input file is identical to the input file for a viscous-CFD three-dimensional mesh. Thus, one obtains the former for free, upon building the latter. Of course, the same sort of model is suitable for a small wind tunnel as well as a small water tunnel, provided that the dynamic pressures are not too high.

12. Laser-Based Distributed-Flowfield Diagnostic Methods

For all of water tunnels' disadvantages *vs*. wind tunnels for aerodynamic testing, water tunnels merit vociferous vindication whenever the research objective is obtaining flowfield data, rather than integrated force/moment on the model. PIV is today's principal experimental technique for obtaining time-resolved, distributed flowfield velocity data -see Willert & Gharib (1991). PIV is considerably easier in water (and in liquids in general) than in air. Water's large density makes distribution and suspension of PIV tracer particles much easier than in air, whereby seeding density is improved, and concomitantly PIV data quality. Particles in water are much more likely to follow the local flow trajectory, especially in high-gradient locales such as vortex cores, than would be the case in wind tunnels. Thus, one occasionally finds PIV wind tunnel data with voids of no-data inside vortex cores, whereas such is demonstrably not the case for water tunnels. Thus one has to carefully weigh the disadvantages of Reynolds-number scaling in water tunnels *vs*. the advantages in PIV.

13. Example: PIV for a UCAV Configuration

Here the motivation was to conduct flowfield velocimetry to understand the fluid mechanics behind force/moment/surface-pressure results obtained in a high-quality test entry in a large industrial-type wind tunnel –see Bruce & Mundel (2003). PIV was not possible for this test, because of the complexity of seeding, of laser power required for such large scales, required alterations to model surface finish (to minimize laser reflection), and of the intractable burdens of equipment setup and data reduction. Pressure-tap data just aft of the wing leading edge on the suction side showed loss of leading-edge suction at outboard stations of the wing,

at angles of attack commensurate with the so-called "pitch break". Was this due to tip stall, or to formation of leading-edge vortices at the model apex or wing/body "juncture"? The hypothesis is that the wingtips stall, losing loading, resulting in a nose-up pitching moment due to sweepback. To verify or to refute this, we need knowledge on whether the wingtips indeed stall at the pitch-break angle of attack, while further inboard the flow remains attached. This requires flowfield information, and was pursued in a water tunnel experiment on a 12-inch-span 3D-printed model of the 1303 UCAV configuration in a water tunnel -see Ol (2006). The wind-and water-tunnel models are shown in Figure 22. The leading edge of the water-tunnel model was "sharp", as far as possible given the manufacturing process.

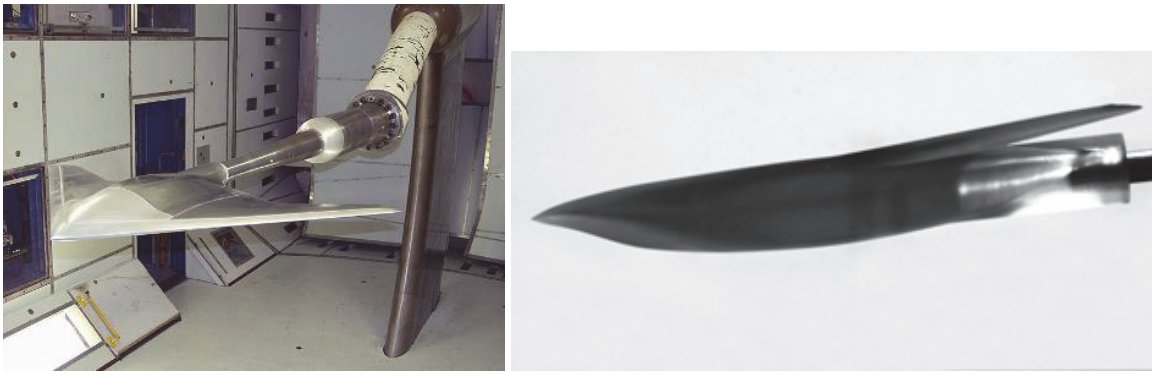

Figure 22. The 1303 UCAV configuration: five-foot-span model installed in QinetiQ 5 m wind tunnel –see Bruce & Mundel (2003), and 3D-printed (plastic) model installed in water tunnel test section –see Ol (2006)

Sectional Reynolds number of the 1303 configuration varied from about 10^4 to 3.2×10^4, depending on the spanwise station. This is clearly in the regime of large flow separations. If fully attached flow is not possible at any angle of attack, then how could one possibly reach a conclusion on the presence or absence of tip stall, and regarding stall at the tips *vs*. further inboard? The answer lies in making reasoned qualitative distinction between a large but *closed* separation, and an *open* separation. This is seen from the comparison of Reynolds stress contours, $u'v'$, shown in Figure 23. For a closed separation, even where the closure occurs in the near-wake, the $u'v'$ distribution will be a characteristic "lobe" pattern just downstream of the trailing edge, with lobes of opposite sign. This is what one sees at the 30% semispan spanwise station at the pitch-break angle of attack, $\alpha = 6^o$. In fact here the $u'v'$ contour is characteristic of a usual airfoil laminar separation bubble, terminating with free shear-layer transition and reattachment just ahead of the trailing edge. At the 90% semispan spanwise station, at $\alpha = 6^o$ the flow is in contrast seen to be fully separated, with an open separation. But at $\alpha = 4^o$ at the same location, one sees a closed separation, evinced by the $u'v'$ double-lobes. This is convincing evidence that the wingtips undergo stall between $\alpha = 4^o$ and $\alpha = 6^o$, while further inboard the flow remains attached. Similar results (not shown here) suggest the absence of a discernable leading-edge-vortex structure, whence we conclude that the pitch-break is due to loss of lift outboard on this highly-tapered cranked-wing configuration, and that a vortex-related process is not a primary cause. Thus, despite the huge disparity in Reynolds number between wind tunnel and water tunnel, the latter gives a good qualitative explanation for flowfield phenomena speculated but not measured in the former.

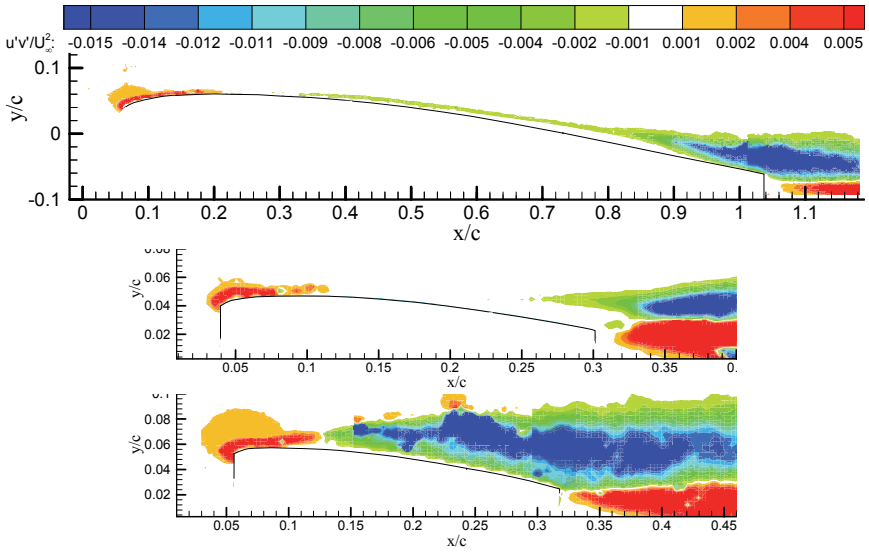

Figure 23. 1303 UCAV water tunnel PIV, contours of Reynolds stress u'v': 30% semispan, a = 6º (top); 90% semispan, a = 4º (middle); and 90% semispan, a = 6º (bottom).

14. General Discussion and Concluding Remarks

Using models in wind and water tunnels to obtain data applicable to full-size vehicles is an inexact science. Reynolds and Mach numbers on models in tunnels can be several orders of magnitude different from those on full-size vehicles, and for tunnel data to be useful, it is essential that the dominant flow characteristics and scaled loads on models are similar to those for full-size vehicles. Although tests in tunnels have been successfully used over the years to obtain much useful information, testing does have its limitations. Data being measured may be dependent on Reynolds numbers and Mach numbers that cannot be achieved by a given tunnel. For example, water tunnels are unsuitable for acquiring aerodynamic data where Mach-number (compressibility) effects are important. Researchers need to have a thorough understanding of the physics of the flow and should always proceed with caution when testing in tunnels.

Due to practical considerations, most testing of models in tunnels is done at Reynolds numbers that are less (often substantially) than the Reynolds numbers on full-size vehicles. An assumption is often made that tunnel data applies to full-size vehicles, even though the Reynolds numbers may be significantly different for the two cases. Alternatively, tunnel data are often extrapolated to apply to full-size vehicles, which is not always straightforward. Wind tunnels used when developing vehicles have Reynolds numbers that are at least an order of magnitude less than those for full-size vehicles, thereby requiring significant extrapolations which are often of questionable accuracy. This applies particularly to flight conditions at high angles of attack involving complicated separated flow patterns with strong vortex interactions. There are not any clear-cut answers on the way to proceed. Munro *et al.* (2005), indicate that Reynolds-number effects do not scale linearly, and that testing at higher Reynolds numbers is not necessarily an advantage. For example, although Reynolds numbers

for tests carried out using a full-size model in the NASA Ames 40 ft by 120 ft tunnel may be lower than those associated with testing a smaller model at a higher velocity in another tunnel, the former experiments can give better results. Smaller models often lack geometric fidelity due to manufacturing constraints and this can cause problems. Tests carried out at a given Reynolds number, but with the Reynolds number obtained using different combinations of variables, do not necessarily give the same results. For example, tests carried out in a given wind tunnel using an aircraft model at a particular free-stream velocity may give significantly different results compared with using a model twice as large but with testing done at half the velocity. Techniques used by say aircraft companies to extrapolate data are often proprietary, making it difficult for researchers to be fully informed of useful extrapolation techniques.

In any small-scale facility, water or air, the small size of models will result in inferior manufacturing tolerances and inability to capture configuration features in detail. For detail-sensitive flowfields, such as separation from some aircraft and missile forebodies, the loss of geometric fidelity incurred with small models may have profound impact on the resulting flowfield, possibly leading to erroneous conclusions. It is therefore crucial that there is consultation between tunnel-practitioners and the airplane-design community, and a water-tunnel test campaign should not be scheduled as an ancillary process to be fitted-in ad hoc.

Boundary layers on water-tunnel models are generally laminar, whereas those on full-size vehicles are almost entirely turbulent, so that the drag forces measured in a water tunnel do not scale with Reynolds number. There is no point measuring axial forces with a water-tunnel balance, and accordingly such balances are usually restricted to five components. Stimulators have been used successfully in wind tunnels to trip laminar boundary layers so that they become turbulent, but stimulators are ineffective in water tunnels since laminar separation would most likely occur.

An analysis of the literature indicates that the location of vortex breakdown over delta wings for different angles of attack can vary substantially for different investigations. Rather than attribute the variations to differences in Reynolds numbers, they are thought to be primarily due to other factors, including different leading edges on the delta wings, tunnel blockages, model support systems, and free-stream conditions. Although flow patterns over delta wings may vary significantly with Reynolds number for different investigations, the global loads measured on models agree more closely. Loads measured and flow patterns captured in water tunnels for models with rounded leading edges do not scale well to full-size vehicles, due to different types of boundary layers and separation locations for the two cases. Consequently, incremental loads on the rounded nose portions of aircraft will be inaccurate and will have an adverse effect on the accuracy of overall measured loads. When models of an F/A-18 aircraft are tested in water tunnels, acquired normal-force coefficients and images of the flow agree well with data for a full-size aircraft. However, this may in fact be fortuitous, since the greater viscous effects in a water tunnel compared with an aircraft in flight counteract the effects of lower Mach numbers in a water tunnel. Whether or not such a situation applies to other aircraft is a matter of conjecture.

The suitability of water tunnels for testing given models needs to be assessed on a case-by-case basis. Water tunnels will not obviate large-scale, high-precision industrial-type testing, and are at most marginally useful for producing reliable results in configuration

aerodynamics, even in the conceptual design stage. For conventional aircraft configuration testing, such as drag-polar measurements, they compare unfavourably to similar-sized wind tunnels, because the latter produce much larger operating Reynolds numbers at the same model scale. Broadly, water tunnels are a powerful tool for basic discoveries in fluid mechanics; problems of bluff bodies, jets/wakes/shear layers, cavities, oscillating bodies and plates, boundary layers and so forth. They are more of a fundamental research tool than an applied aerodynamics tool. However, they are eminently useful as part of a larger solution space, by focusing the test matrix in large wind tunnels and providing validation for CFD. This is especially true when equipped with modern optical-flowfield-velocimetry techniques, such as PIV, which is much easier to implement in water tunnels than in wind tunnels. Using water tunnels, it is possible to simultaneously measure loads and visualise high-quality off-surface flows, so that the loads and images can be correlated directly.

In problems insensitive to Reynolds number, or where Reynolds number between the application and the water tunnel test article are closely matched, water tunnels should be regarded as the useful tool of experimental aerodynamics. An example is laminar-separation-bubble and boundary-layer-transition experiments on a Selig SD7003 airfoil, where water tunnel, wind tunnel and tow tank produced similar results –see Ol *et al.* (2005). Water tunnels do have particular strengths in some practical aeronautical engineering applications even at the detailed-design level. These are principally those cases where the full-scale Reynolds number is itself low or is otherwise unimportant. For the former, two examples are some cases in turbine blades, and the emerging area of Micro Air Vehicles (MAVs). For the latter, sharp-edged swept wings are perhaps the most celebrated example, though not without controversy. Dynamic stall is another example.

Dynamic testing has been suggested as an application particularly amenable to water-tunnel testing, because of the favourable scaling of physical motion frequencies in liquid flows. While this is broadly true, the conclusion must be qualified by the kind of dynamic testing that one has in mind. For high-rate and/or high-angle-of-attack problems, the utility of water tunnels is demonstrably obvious. But for conventional dynamic-derivative measurements for airplane configurations, we recommend withholding judgment until a definitive test is conducted. This would be a common experiment in a water tunnel and a large wind tunnel, running the same configuration at the same rates and the same motion kinematics. At DSTO, dynamic tests in a water tunnel using a Standard Dynamics Model have shown that measured aerodynamic derivatives are as acceptable, i.e. no better or no worse, than corresponding wind-tunnel data.

15. Acknowledgements

The authors are grateful to support staff at AFRL and DSTO, who made many helpful suggestions.

16. References

Alemdaroglu, N., Iyigun, I., Altun, M., Quagliotti, F. & Guglieri, G. 2001 Measurements of dynamic stability derivatives using direct forced oscillation technique. Instrumentation in Aerospace Simulation Facilities, *19th International Congress on Instrumentation in Aerospace Simulation Facilities*, Cleveland, OH, USA, Aug.

Atashbaz, G. & Ahmed, N. A. 1997 Asymmetry of vortex flow over slender delta wings. *International Aerospace Congress 97*, Sydney, Australia, 24-27 Feb.

Beyers, M. E. 1985 SDM pitch- and yaw-axis stability derivatives. Paper 1985-1827, *AIAA Atmospheric Flight Mechanics Conference*, Snowmass, CO, USA, Aug.

Beyers, M. & Ericsson, L. 2001 Why is LEX vortex breakdown on the F/A-18 configuration insensitive to Reynolds number? Paper 2001-0690, *AIAA 39th Aerospace Sciences Meeting and Exhibit*.

Beyers, M. E., Kapoor, K. B. & Moulton, B. E. 1984 Pitch- and yaw-oscillation experiments on the Standard Dynamics Model at Mach 0.6. National Research Council Canada, National Aeronautical Establishment, *Report LTR-UA-76*, Jun.

Brandon, J. M. & Shah, G. H. 1990 Unsteady aerodynamic characteristics of a fighter model undergoing large-amplitude pitching motions at high angles of attack. Paper 90-0309, *AIAA 28th Aerospace Sciences Meeting*, Reno, NV, USA, Jan.

Bruce, R. J. & Mundell, A. R. G. 2003 Low Speed Wind Tunnel Tests on the 1303 UCAV Concept. *QinetiQ/FST/TR025502/1.0,* QinetiQ Ltd., Farnborough, UK, Mar.

Chapman, G. T. & Keener, E. R. 1979 Aerodynamics of bodies of revolution at angle of attack to 90°. AIAA Paper 79-0023.

Cunningham, A. M. Jr. & Bushlow, T. 1990 Steady and unsteady force testing of fighter aircraft models in a water tunnel. Paper 90-2815-CP, *AIAA 8th Applied Aerodynamics Conference*, Portland, OR, USA, Aug.

Cyran, F. B. 1981 Sting interference effects on the static, dynamic, and base pressure measurements of the Standard Dynamics Model aircraft at Mach numbers 0.3 through 1.3. Arnold Engineering Development Center, *Report AEDC-TR-81-3*, Aug.

Earnshaw, P. B. & Lawford, J. A. 1966 Low-speed wind-tunnel experiments on a series of sharp-edged delta wings. *Aeronautical Research Council, R&M 3424*.

Elle, B. J. 1958 An investigation at low speed of the flow near the apex of thin delta wings with sharp leading edges. *Aeronautical Research Council, R&M 3176*.

Erickson, G. E. 1981 Vortex flow correlation. *Air Force Wright Aeronautical Laboratories TR-80-3143*.

Erickson, G. E., Hall, R. M., Banks, D. W., Del Frate, J. H., Schreiner, J. A., Hanley, R. J. & Pulley, C. T. 1989 Experimental investigation of the F/A-18 vortex flows at subsonic through transonic speed. Paper 89-2222 (invited), *AIAA 7th Applied Aerodynamics Conference*, Seattle, WA, USA.

Erm, L. P. 2003 Measurement of flow-induced pressures on the surface of a model in a flow-visualization water tunnel. *Experiments in Fluids*, Vol. 35, Number 6.

Erm, L. P. 2006a Development of a two-component strain-gauge-balance load-measurement system for the DSTO water tunnel. *DSTO-TR-1835*, Platforms Sciences Laboratory, Defence Science and Technology Organisation, Melbourne, Australia.

Erm, L. P. 2006b Development of a dynamic testing capability for the DSTO water tunnel. *DSTO-TR-1836*, Platforms Sciences Laboratory, Defence Science and Technology Organisation, Melbourne, Australia.

Erm, L. P. 2011 An experimental investigation into the feasibility of measuring static and dynamic aerodynamic derivatives in the DSTO water tunnel. *DSTO-TR-2600*, Defence Science and Technology Organisation, Melbourne, Australia.

Erm, L. P. & Ferrarotto, P. 2010 Development of a five-component strain-gauge balance for the DSTO water tunnel. *DSTO-GD-0597*, Defence Science and Technology Organisation, Melbourne, Australia.

Etkin, B. 2005 Dynamics of Atmospheric Flight. Dover Publications, New York.

Fisher, D. F. & Cobleigh, B. R. 1994 Controlling forebody asymmetries in flight –experience with boundary layer transition strips. Paper 94-1826, *AIAA 12th Applied Aerodynamics Conference*.

Goertz, S. 2002 Steady and unsteady CFD simulations of vortex breakdown over swept delta wings. Royal Institute of Technology, Sweden, September.

Guglieri, G. & Quagliotti, F. B. 1991 Determination of dynamic stability parameters in a low speed wind tunnel. Paper 91-3245-CP, *AIAA 9th Applied Aerodynamics Conference*, Baltimore, MD, USA, Sep.

Hartmann, K. 1978 Ueber den einfluss der Reynoldzahl auf die normalkraefte schlanker flugkoerperruempfe. *Zeitschrift fur Flugwissenschaften und Weltraumforschung*, Vol. 2, No. 1.

Holze, C., Oelze, H. W. & Rath, H. J. 2002 Pressurised temperature-variable water tunnel for high Reynolds number research. Paper 2002-0701, AIAA 40th Aerospace Sciences Meeting & Exhibit.

Huang, X. Z. & Beyers, M. E. 1990 Subsonic aerodynamic coefficients of the SDM at angles of attack up to 90°. National Research Council Canada, National Aeronautical Establishment, *Report LTR-UA-93*, Jan.

Jarrah, M-A. M. 1989 Low-speed wind-tunnel investigation of the flow about delta wing, oscillating in pitch to very high angle of attack. Paper 89-0295, *AIAA 27th Aerospace Sciences Meeting*.

Kabin, S. V., Kolinko, K. A., Khrabrov, A. N. & Nushtaev, P. D. 1995 Dynamic test rig and test technique for the aircraft models unsteady aerodynamic characteristics measurements in high subsonic and transonic wind tunnels. *International Congress on Instrumentation in Aerospace Simulation Facilities, ICIASF '95 Record*.

Kaplan, S. M., Altman, A., and Ol, M. 2007 Wake vorticity measurements for low aspect ratio wings at low Reynolds number. *J. Aircraft*, Vol. 44, No. 1.

Kohlman, D. L. & Wentz, W. H. Jr. 1971 Vortex breakdown on slender sharp-edged wings. *J. Aircraft*, Vol. 8, No. 3.

Kowal, H. & Vakili, A. 1998 An investigation of unsteady vortex flow for a pitching-rolling 70° delta wing. Paper 98-0416, *AIAA 36th Aerospace Sciences Meeting and Exhibit*.

Kramer, B. R. 2002 Experimental Evaluation of Superposition Techniques Applied to Dynamic Aerodynamics. Paper 2002-0700, *AIAA 40th Aerospace Sciences Meeting & Exhibit*.

Kramer, B. R., Malcolm, G. N., Suarez, C. J. & James, K. D. 1994 Pressure distributions around an F/A-18, in static and rotary flow fields, with forebody vortex control. Paper 94-1828, *AIAA 12th Applied Aerodynamics Conference.*

Kramer, B. R., Suarez, C. J., Malcolm, G. N. & Ayres, B. F. 1993 F/A-18 forebody vortex control. *Eidetics TR-93-003* Volume I (Static Tests), Apr.

Lamont, P. J. 1982 The complex asymmetric flow over a 3.5D ogive nose and cylindrical afterbody at high angles of attack. Paper 82-0053, AIAA 20th Aerospace Sciences Meeting

Lanser, W. R. & Murri, D. G. 1993 Wind tunnel measurements on a full-scale F/A-18 with forebody slot blowing or forebody strakes. Paper 93-1018, *AIAA/AHS/ASEE Aerospace Design Conference*, Irvine, CA USA.

Lawford, J. A. & Beauchamp, A. R. 1963 Low-speed wind-tunnel measurements on a thin sharp-edged delta wing with 70° leading-edge sweep, with particular reference to the position of leading-edge-vortex breakdown. *Aeronautical Research Council, R&M 3338*.

LeMay, S. P., Batill, S. M. & Nelson, R. C. 1990 Vortex dynamics on a pitching delta wing. *J. Aircraft*, Vol. 27., No. 2, Feb.

Lowson, M. V. & Riley, A. J. 1994 Vortex breakdown control by delta wing geometry. Paper 94-3487-CP, AIAA 19th Atmospheric Flight Mechanics Conference.

McKernan, J. F. 1983 An investigation of the breakdown of the leading edge vortices on a delta wing at high angles of attack. Master of Science in Aerospace Engineering, Department of Aerospace and Mechanical Engineering, University of Notre Dame, Notre Dame, IN, USA.

McKernan, J. F. & Nelson, R. C. 1983 An investigation of the breakdown of the leading edge vortices on a delta wing at high angles of attack. Paper 83-2114, *AIAA 10th Atmospheric Flight Mechanics Conference*.

Miau, J. J., Chang, R. C., Chou, J. H. & Lin, C. K. 1992 Nonuniform motion of leading-edge vortex breakdown on ramp pitching delta wings. *AIAA Journal*, Vol. 30.

Mitchell, A., Barberis, D. & Delery, J. 1998 Oscillation of vortex breakdown location and its control by tangential blowing. Paper 98-2914, *AIAA 29th Fluid Dynamics Conference*.

Mueller, T. J. & DeLaurier, J. D. 2001 An Overview of Micro Air Vehicle Aerodynamics. Fixed and Flapping Wing Aerodynamics for Micro Air Vehicle Applications, T.J. Mueller, ed., *Progress in Astronautics and Aeronautics*, Vol. 195, Published by AIAA.

Munro, C., Jouannet, C. & Krus, P. 2003 Flow visualisation and force and moment correlations in a water tunnel. 7th *Triennial International Symposium on Fluid Control, Measurement and Visualization, FLUCOME 2003*, Sorrento, Italy.

Munro, C. D., Krus, P. & Jouannet, C. 2005 Implications of scale effect for the prediction of high angle of attack aerodynamics. *Progress in Aerospace Sciences*, Vol. 41.

Munsen, B. R., Young, D. F. & Okiishi, T. H. 2006 Fundamentals of fluid mechanics, Fifth Edition, John Wiley & Sons, Incorporated.

Ol, M. V. 2006 Water Tunnel Velocimetry Results for the 1303 UCAV Configuration. Paper 2006-2990, *AIAA 24th Applied Aerodynamics Conference*.

Ol, M. V., McCauliffe, B. R., Hanff, E. S., Scholz, U. & Kaehler, C. 2005 Comparison of Laminar Separation Bubble Measurements on a Low Reynolds Number Airfoil in Three Facilities. Paper 2005-5149, *AIAA 35th Fluid Dynamics Conference and Exhibit*.

Payne, F. M. 1987 The structure of leading edge vortex flows including vortex breakdown. PhD thesis, University of Notre Dame, Notre Dame, IN, USA.

Phillis, D. L. 1991 Force and pressure measurements over a 70^o delta wing at high angles of attack and sideslip. Masters Thesis, Aeronautical Engineering Department, The Wichita State University, USA.

Polhamus, E. C. 1984 A review of some Reynolds Number effects related to bodies at high angles of attack. *NASA Contractor Report 3809*.

Rizzi, A., Goertz, S. & Munukka, K. 1999 Computational study of vortex breakdown over swept delta wings. Paper 99-3118, *AIAA 17th Applied Aerodynamics Conference*.

Roos, F. W. & Kegelman, J. T. 1990 An experimental investigation of sweep-angle influence on delta-wing flows, Paper 90-0383, *AIAA 28th Aerospace Sciences Meeting*, Reno, NV, USA, Jan.

Schmidt, E. 1985 Standard Dynamics Model experiments with the DFVLR/AVA transonic derivative balance. *AGARD-CP-386*, *Unsteady Aerodynamics –Fundamentals and Applications to Aircraft Dynamics*.

Selig, M., *et al*. 2006-2008 Private communications.

Soltani, M. R., Bragg, M. B. & Brandon, J. M. 1988 Experimental measurements on an oscillating 70-degree delta wing in subsonic flow. *Paper 88-2576-CP, AIAA 6th Applied Aerodynamics Conference*.

Soria, J., New, T.H., Lim, T.T. & Parker, K. 2003 Multigrid CCDPIV measurements of accelerated flow past an airfoil at an angle of attack of 30^o. *Exp. Thermal and Fluid Science*, Vol. 27.

Suárez, C. J., Ayers, B. F. & Malcolm, G. N. 1994 Force and moment measurements in a flow visualisation water tunnel. Paper 94-0673, *AIAA 32nd Aerospace Sciences Meeting and Exhibit*.

Suárez, C. & Malcolm, G. 1994 Water tunnel force and moment measurements on an F/A-18. Paper 94-1802, *AIAA 12th Applied Aerodynamics Conference*, Colorado Springs, CO, USA, Jun.

Suárez, C. J., Malcolm, G. N., Kramer, B. R., Smith, B. C. & Ayers, B. F. 1994 Development of a multicomponent force and moment balance for water tunnel applications, Volumes I and II. *NASA Contractor Report 4642*.

Thompson, D. H. 1990 Water tunnel flow visualization of vortex breakdown over the F/A-18. *Flight Mechanics Report 179*, Aeronautical Research Laboratory, Defence Science and Technology Organisation, Melbourne, Australia.

Traub, L. W., Moeller, B. & Rediniotis, O. 1998 Low-Reynolds-number effects on delta-wing aerodynamics. *J. Aircraft*, Vol. 35, No. 4.

Ueno, M. & Miwa, H. 2001 New dynamic stability equipment for transonic wind tunnel testing at NAL. Paper 2001-0406, *39th AIAA Aerospace Sciences Meeting and Exhibit*, Reno, NV, USA, Jan.

Wentz, W. H. Jr. & Kohlman, D. L. 1968 Wind tunnel investigation of vortex breakdown on slender sharp-edged wings. *Technical Report FRL 68-013*, University of Kansas Center for Research, Lawrence, KS, USA.

Willert, C.E. & Gharib, M. 1991 Digital Particle Image Velocimetry. *Experiments in Fluids*, Vol. 10, No. 4, Jan.

Williams, D. R., Collins, J., Tadmor, G. & Colonius, T. 2008 Control of a semi-circular planform wing in a "gusting" unsteady freestream flow: I-Experimental issues. Paper 2008-3976, *AIAA 38th Fluid Dynamics Conference and Exhibit*.

DEFENCE SCIENCE AND TECHNOLOGY ORGANISATION
DOCUMENT CONTROL DATA

1. PRIVACY MARKING/CAVEAT (OF DOCUMENT)

2. TITLE

An Assessment of the Usefulness of Water Tunnels for Aerodynamic Investigations

3. SECURITY CLASSIFICATION (FOR UNCLASSIFIED REPORTS THAT ARE LIMITED RELEASE USE (L) NEXT TO DOCUMENT CLASSIFICATION)

Document	(U)
Title	(U)
Abstract	(U)

4. AUTHOR(S)

Lincoln P. Erm and Michael V. OL

5. CORPORATE AUTHOR

DSTO Defence Science and Technology Organisation
506 Lorimer St
Fishermans Bend Victoria 3207 Australia

6a. DSTO NUMBER	6b. AR NUMBER	6c. TYPE OF REPORT	7. DOCUMENT DATE
DSTO-TR-2803	AR-015-530	Technical Report	December 2012

8. FILE NUMBER	9. TASK NUMBER	10. TASK SPONSOR	11. NO. OF PAGES	12. NO. OF REFERENCES
2008/1098697/1	07/250	DSTO, AFRL	38	67

13. DSTO Publications Repository

http://dspace.dsto.defence.gov.au/dspace/

14. RELEASE AUTHORITY

Chief, Air Vehicles Division

15. SECONDARY RELEASE STATEMENT OF THIS DOCUMENT

Approved for public release

OVERSEAS ENQUIRIES OUTSIDE STATED LIMITATIONS SHOULD BE REFERRED THROUGH DOCUMENT EXCHANGE, PO BOX 1500, EDINBURGH, SA 5111

16. DELIBERATE ANNOUNCEMENT

No Limitations

17. CITATION IN OTHER DOCUMENTS Yes

18. DSTO RESEARCH LIBRARY THESAURUS

Water tunnels, Aircraft models, Fluid dynamics, Reynolds number, Load tests

19. ABSTRACT

Water tunnels are emerging as a possible useful alternative to small low-speed wind tunnels for an expanded range of aerodynamic testing. In this report, an assessment is made regarding the extent to which water tunnels can be used for such testing. It was found that their suitability for testing given models needs to be assessed on a case-by-case basis. For conventional tests on aircraft, such as force and moment measurements, they compare unfavourably with similar-sized wind tunnels, due to a mismatch in Reynolds numbers. Water tunnels are generally better suited to carrying out fundamental research than they are for applied aerodynamics testing. However, they are very useful as part of a large research program, by helping establish the testing schedule for large wind tunnels. In flow situations that are insensitive to Reynolds number, or where a test Reynolds number is close to that of a full-size vehicle, water tunnels should be regarded as the preferred option for experimental aerodynamics. Such examples include micro air vehicles, high-rate dynamic testing, and high-sweep sharp-edge configurations. Water tunnels are also very useful for providing validation data for computational-fluid-dynamics analyses of a flow. An earlier version of this work was prepared for the TTCP TR-AER-TP5 Panel in August 2010.